

Robust and efficient data-driven predictive control

Mohammad Alsalti*, Manuel Barkey*, Victor G. Lopez, Matthias A. Müller

Leibniz University Hannover, Institute of Automatic Control, 30167 Hannover, Germany

Abstract

We propose a robust and efficient data-driven predictive control (eDDPC) scheme which is more sample efficient (requires less offline data) compared to existing schemes, and is also computationally efficient. This is done by leveraging an alternative data-based representation of the trajectories of linear time-invariant (LTI) systems. The proposed scheme relies only on using (short and potentially irregularly measured) noisy input-output data, the amount of which is independent of the prediction horizon. To account for measurement noise, we provide a novel result that quantifies the uncertainty between the true (unknown) restricted behavior of the system and the estimated one from noisy data. Furthermore, we show that the robust eDDPC scheme is recursively feasible and that the resulting closed-loop system is practically stable. Finally, we compare the performance of this scheme to existing ones on a case study of a four tank system.

Key words: Robust data-driven predictive control, behavioral approach, uncertainty quantification, SVD perturbations.

1 Introduction

Model predictive control (MPC) [1] is a powerful optimization-based control technique that is applicable to multivariable linear and nonlinear systems, handles hard constraints on the input, state and output while minimizing a certain performance criterion. MPC uses a model of the system being controlled in order to predict the behavior of the system over a finite horizon. For complex systems that are difficult to model from first principles, sufficiently accurate models can be obtained using machine learning techniques. This has led to the development of learning-based predictive control schemes, with accompanying closed-loop guarantees (see, e.g., [2]). Such schemes are indirect, since they rely on first learning a model from data.

Direct data-driven predictive control (DDPC) schemes have recently been developed using results from the behavioral approach to systems theory [3]. There, non-parametric representations given by the image of data matrices (see, e.g., [4, 5]) are employed as predictive

“models” (cf. [6]). Open-loop robustness and closed-loop guarantees of DDPC schemes for LTI systems were established in [7–9]. Many extensions soon followed including nonlinear [10–14], stochastic [15, 16] and distributed DDPC [17, 18] among others. To account for noisy data, different regularization techniques were proposed (see, e.g., [19, 20] and the references therein). DDPC schemes have also been successfully applied to various real-world systems, e.g., power systems [21], quadcopters [22] and many others, thus making DDPC an important and well-established control technique. We refer to [23] for a comprehensive survey of DDPC and its extensions.

Successful application of DDPC schemes requires that the collected offline data is sufficiently rich. This is typically ensured by imposing suitable persistence of excitation (PE) conditions on the input. However, PE necessitates that the data sequence is sufficiently long and its length increases with increased system order, number of inputs and prediction horizon length. As a result, the computational complexity of solving the corresponding optimal control problem increases. Existing works that address efficiency in DDPC either focus on sample efficiency (using less data) by, e.g., segmentation of the prediction horizon [24], or on computational efficiency by reducing the number of decision variables through the use of, e.g., singular value decomposition (SVD) of the data matrices [25]. None of the above schemes, however, simultaneously addresses sample and computational efficiency of DDPC schemes. In fact, the segmentation procedure in [24] results in an increased number of de-

* M. Alsalti and M. Barkey contributed equally to this work. Parts of this paper have been presented at the 2024 European Control Conference, June 25-28, 2024, Stockholm, Sweden. Corresponding author: Mohammad Alsalti.

Email addresses: alsalti@irt.uni-hannover.de (Mohammad Alsalti*), barkey@irt.uni-hannover.de (Manuel Barkey*), lopez@irt.uni-hannover.de (Victor G. Lopez), mueller@irt.uni-hannover.de (Matthias A. Müller).

cision variables, whereas [25] requires the availability of a sufficiently long data sequence. In some practical applications, it may not be easy to obtain long PE data that allow for application of DDPC schemes with long prediction horizons. Moreover, data can be irregularly measured due to sensor failure or inability to measure data consecutively (as in, e.g., biomedical applications). It was recently shown in [26] how one can obtain alternative non-parametric representations of the finite-length behavior of LTI systems using a (potentially short and irregularly measured) data sequence. In this work, we will exploit the results of [26] to simultaneously address sample- and computational efficiency issues in DDPC.

Contributions: First, we propose a sample- and computationally-efficient robust data-driven predictive control (eDDPC). Unlike existing methods, this scheme can also potentially be employed when only short and irregularly measured (noisy) data is available. In the preliminary conference version of this work (see [27]), we presented the nominal noise-free setting. To account for measurement noise, we provide as a second contribution a novel result on uncertainty quantification in the behavioral framework. In particular, we derive a bound on the angle between two subspaces: the unknown finite-length behavior of the system and its known approximation. Our results rely on investigating SVD perturbations of the data matrices (cf. [28]). In contrast, existing works on uncertainty quantification in the behavioral framework [29, 30] measure the distance between two *known* behaviors. As a third contribution, we show that the robust eDDPC scheme is recursively feasible and that the closed-loop system is practically stable. This is different from existing efficient DDPC schemes (e.g., [24, 25]) where no recursive feasibility and/or robust stability guarantees were provided. Finally, we analytically and numerically (using a case study of a four tank system) compare the performance of this scheme to existing ones from the literature.

Section 2 introduces the notation and necessary preliminaries. Section 3 presents the nominal eDDPC scheme. Section 4 includes a novel result on uncertainty quantification in the behavioral framework. Section 5 formulates the robust eDDPC scheme in presence of noise and establishes stability guarantees. Section 6 includes a simulation case study and Section 7 concludes the paper.

2 Preliminaries

The sets of integers, natural and real numbers are denoted by \mathbb{Z} , \mathbb{N} , \mathbb{R} , respectively. The restriction of integers to an interval is denoted by $\mathbb{Z}_{[a,b]}$ for $b > a \in \mathbb{Z}$. For a matrix $M \in \mathbb{R}^{m \times n}$, we denote its image by $\text{im}(M)$ and its kernel by $\ker(M)$. When a basis of $\ker(M)$ is to be computed, we write $N = \text{null}(M)$ which returns a matrix N of appropriate dimensions such that $MN = 0$. The singular values of the matrix M are ordered scalars denoted

by $s_1(M) \geq s_2(M) \geq \dots \geq s_{\min\{m,n\}}(M) \geq 0$. We use $\|M\|_i$, $i \in \{2, \infty, F\}$, to denote the induced norms or the Frobenius norm, respectively. For two matrices $M_1 \in \mathbb{R}^{n_1 \times n_2}$ and $M_2 \in \mathbb{R}^{n_3 \times n_4}$, we denote by $\text{diag}(M_1, M_2) = \begin{bmatrix} M_1 & 0_{n_1 \times n_4} \\ 0_{n_3 \times n_2} & M_2 \end{bmatrix}$. For a symmetric positive definite matrix $P = P^\top \succ 0$, we denote its largest (respectively, smallest) eigenvalue by $\lambda_{\max}(P)$ ($\lambda_{\min}(P)$). We define the weighted norm of a vector x as $\|x\|_P := \sqrt{x^\top P x}$. In contrast, $\|x\|_i$, $i \in \{1, 2, \infty\}$, denotes the standard vector norms. A function $\phi : \mathbb{R}_{\geq 0} \rightarrow \mathbb{R}_{\geq 0}$ is said to be of class \mathcal{K}_∞ if it is continuous, zero at zero, strictly increasing and $\lim_{r \rightarrow \infty} \phi(r) = \infty$.

For $T \in \mathbb{N}$, the set of finite-length q -variate, real-valued time series $w = (w_0, w_1, \dots, w_{T-1})$ is denoted by $(\mathbb{R}^q)^T$. With slight abuse of notation, we also use w to denote the stacked vector $w = [w_0^\top \ w_1^\top \ \dots \ w_{T-1}^\top]^\top \in \mathbb{R}^{qT}$, and a window of it by $w_{[a,b]}$ where $0 \leq a < b \leq T-1$. The Hankel matrix of depth $L \leq T$ of w is defined as

$$\mathcal{H}_L(w) = \begin{bmatrix} w_{[0,L-1]} & w_{[1,L]} & \dots & w_{[T-L,T-1]} \end{bmatrix}.$$

The (finite-length) behavior $(\mathcal{B}|_T)$ \mathcal{B} of a dynamical system is defined as a set of (finite-) infinite-length trajectories (cf. [3]). Let $u_t \in \mathbb{R}^m$ and $y_t \in \mathbb{R}^p$ denote the inputs and outputs of a system at time t , and define a partitioning of $w_t \in \mathbb{R}^q$ such that $w_t = \begin{bmatrix} u_t \\ y_t \end{bmatrix}$. A trajectory of length T of the system is denoted by $w \in \mathcal{B}|_T$. The set of discrete-time LTI systems with q variables and known¹ complexity (m, n, ℓ) is denoted by $\partial\mathcal{L}_{m,n,\ell}^q$, where $q = m + p$ and (m, n, ℓ) denote (i) the number of inputs, (ii) the order of the system, and (iii) the lag of the system (observability index), respectively.

A *kernel representation* of $\mathcal{B} \in \partial\mathcal{L}_{m,n,\ell}^q$ is given by [3]

$$\mathcal{B} = \ker(R(\sigma)) = \{w : \mathbb{N} \rightarrow \mathbb{R}^q \mid R(\sigma)w = 0\}, \quad (1)$$

where $\sigma^j w(k) := w(k+j)$, for $j \in \mathbb{N}$, is the shift operator and $R(\sigma)$ is defined by the polynomial matrix

$$R(z) = \begin{bmatrix} r_1(z) \\ \vdots \\ r_g(z) \end{bmatrix} = \begin{bmatrix} r_{1,0} + r_{1,1}z + \dots + r_{1,\ell_1}z^{\ell_1} \\ \vdots \\ r_{g,0} + r_{g,1}z + \dots + r_{g,\ell_g}z^{\ell_g} \end{bmatrix}, \quad (2)$$

with $r_{i,j} \in \mathbb{R}^{1 \times q}$. Given a trajectory $w \in \mathcal{B}|_T$ of an LTI system $\mathcal{B} \in \partial\mathcal{L}_{m,n,\ell}^q$, it holds by linearity and shift-invariance that $\text{im}(\mathcal{H}_L(w)) \subseteq \mathcal{B}|_L$. When equality holds, we obtain a data-based representation of the finite-length behavior of the system (see [5] for more

¹ When only an upper bound on n is known, inferring the true system's order from data is possible under certain conditions, e.g., noise-free data or high signal-to-noise ratio. For simplicity, we consider systems of known complexity.

details). For controllable systems, persistence of excitation (see Definition 1 below) of the input ensures that $\text{im}(\mathcal{H}_L(w)) = \mathcal{B}|_L$ [4]. This is known as the *fundamental lemma* and is formally stated in Lemma 1 below.

Definition 1 [4] *A sequence $u \in (\mathbb{R}^m)^T$ is said to be persistently exciting of order L if $\text{rank}(\mathcal{H}_L(u)) = mL$.*

Lemma 1 [4] *Let $w \in \mathcal{B}|_T$ with $\mathcal{B} \in \partial\mathcal{L}_{m,n,\ell}^q$ controllable. For $L \geq \ell$, let $u \in (\mathbb{R}^m)^T$ be PE of order $L+n$, then*

$$\text{rank}(\mathcal{H}_L(w)) = mL + n, \quad (3)$$

and $\bar{w} \in \mathcal{B}|_L$ if and only if $\exists \alpha \in \mathbb{R}^{T-L+1}$ such that

$$\mathcal{H}_L(w)\alpha = \bar{w}. \quad (4)$$

Another result which follows from the rank condition (3) is *identifiability from data* which allows us to retrieve a kernel representation (2) from data. This is formalized in the following corollary (see also [5]).

Corollary 2 [26, Cor. 2] *Given $w \in \mathcal{B}|_T$ where $\mathcal{B} \in \partial\mathcal{L}_{m,n,\ell}^q$, suppose $\text{rank}(\mathcal{H}_d(w)) = md + n$ for $d \geq \ell + 1$. Then, the coefficients of the polynomial matrix $R(\sigma)$ in (2) are given by the rows of $R_d \in \mathbb{R}^{p^{d-n} \times q^d}$ where $R_d = \text{null}(\mathcal{H}_d(w)^\top)^\top$.*

It was further shown in [26] that one can use R_d to obtain a data-based representation (alternative to that in (4)) of the finite-length behavior of the system $\mathcal{B}|_L$. This result is summarized in the following theorem.

Theorem 3 [26, Th. 3, Cor. 3] *Let the conditions of Corollary 2 hold. Then, for any $L \geq d$, $\bar{w} \in \mathcal{B}|_L$ if and only if there exists a vector $\beta \in \mathbb{R}^{mL+n}$ such that*

$$P\beta = \bar{w}, \quad (5)$$

where $P = \text{null}(\Gamma)$ and Γ is given by

$$\Gamma = \begin{bmatrix} r_{1,0} & r_{1,1} & \cdots & r_{1,d-1} \\ r_{2,0} & r_{2,1} & \cdots & r_{2,d-1} \\ \vdots & \vdots & \ddots & \vdots \\ r_{pd-n,0} & r_{pd-n,1} & \cdots & r_{pd-n,d-1} \\ & r_{1,0} & r_{1,1} & \cdots & r_{1,d-1} \\ & r_{2,0} & r_{2,1} & \cdots & r_{2,d-1} \\ & \vdots & \vdots & \ddots & \vdots \\ & r_{p,0} & r_{p,1} & \cdots & r_{p,d-1} \\ & & & & \ddots \\ & & & r_{1,0} & r_{1,1} & \cdots & r_{1,d-1} \\ & & & r_{2,0} & r_{2,1} & \cdots & r_{2,d-1} \\ & & & \vdots & \vdots & \ddots & \vdots \\ & & & r_{p,0} & r_{p,1} & \cdots & r_{p,d-1} \end{bmatrix}, \quad (6)$$

where $r_{i,j} \in \mathbb{R}^{1 \times q}$ are the elements of R_d in Corollary 2.

The results of Theorem 3 and Lemma 1 both provide non-parametric representations of the finite-length behavior of a controllable LTI system. Specifically, any tra-

jectory $\bar{w} \in \mathcal{B}|_L$ can be expressed as a linear combination of the columns of the Hankel matrix or of the matrix P . This is because $\text{im}(\mathcal{H}_L(w)) = \text{im}(P) = \mathcal{B}|_L$. However, there are two important distinctions:

- D1** Theorem 3 requires at least $T \geq (m+1)(\ell+n+1) - 1$ data points to satisfy the PE condition on the input, whereas Lemma 1 requires at least $T \geq (m+1)(L+n) - 1$, which depends on L . If the minimum T is chosen in both cases, then Theorem 3 will always require $(m+1)(L-\ell-1)$ fewer samples, for any $L > \ell + 1$.
- D2** Unlike (4), equation (5) does not result in an over-parameterization of the spanned trajectories. Specifically, for each $\bar{w} \in \mathcal{B}|_L$, (4) has infinitely many solutions for $\alpha \in \mathbb{R}^{T-L+1}$, whereas the corresponding $\beta \in \mathbb{R}^{mL+n}$ vector in (5) is *unique*. Notice that the dimension of β is *independent* from the number of previously collected data, whereas the dimension of α increases with increasing T . In fact, even if the minimum number of data points was chosen for the results of Lemma 1, then the dimension of β in Theorem 3 would still be smaller than the dimension of α by mn .

Remark 4 *Although the results of [26] hold for the general case of irregularly measured data, in this paper we consider for simplicity that the offline data is complete. The results of this work are still applicable for the case of irregularly measured offline data, provided that one can compute R_d from the available measurements (see [26, Th. 4], where successful computation of R_d from irregular measurements can be guaranteed by design of input for certain patterns of missing data). For complete and exact (noise-free) data, one can already obtain R_d for $d = \ell + 1$ if (3) is satisfied (cf. Corollary 2). Later in Section 5 when dealing with noisy data, d assumes the role of a hyperparameter that can be tuned to enhance the performance of the proposed robust eDDPC scheme.*

Remark 5 *Depending on (m, p, ℓ, n) , the matrix Γ in (6) can potentially be numerically ill-conditioned. It was observed that when the p rows of R_d which are shifted in (6) specify a minimal kernel representation of the system, then Γ tends to have a smaller condition number. Reducing a non-minimal kernel representation is a difficult problem and will be pursued elsewhere. In Section 6, we avoid this issue by devising a (heuristic) combinatorial method which tests different combinations of p rows of R_d that result in a low condition number of Γ .*

3 Nominal eDDPC scheme

In this section, we recall results from our preliminary conference version [27] where the eDDPC scheme was presented in the nominal noise-free case. The goal of eDDPC is to stabilize a (known) equilibrium point of the unknown LTI system, while satisfying input-output constraints. Such a point is defined in terms of the system's inputs and outputs as follows.

Algorithm 1. Offline data pre-processing for eDDPC

Input: Measurements $w \in \mathcal{B}|_T$, where $\mathcal{B} \in \partial \mathcal{L}_{m,n,\ell}^q$, satisfying $\text{rank}(\mathcal{H}_d(w)) = md + n$ for $d \geq \ell + 1$.

- 1) Compute $R_d = \text{null}(\mathcal{H}_d(w)^\top)^\top$.
- 2) Use R_d to build Γ as in (6), with $L + n - d$ shifts.
- 3) Obtain $P = \text{null}(\Gamma)$.

Output: Matrix P where $\text{im}(P) = \mathcal{B}|_{L+n}$.

Definition 2 [8] *A point w^s is an equilibrium of $\mathcal{B} \in \partial \mathcal{L}_{m,n,\ell}^q$ if $w' \in (\mathbb{R}^q)^{n+1}$, with $w'_k = w^s$ for all $k \in \mathbb{Z}_{[0,n]}$, is a trajectory of the system, i.e., $w' \in \mathcal{B}|_{n+1}$. We use w_n^s to denote a column vector containing n instances of w^s .*

The eDDPC scheme uses the matrix P (cf. (5)) to make the predictions over the horizon² $L + n$. Recall that Theorem 3 implements a few (algebraic) pre-processing steps on the collected data in order to arrive at the matrix P in (5). In Algorithm 1, we summarize these steps which can be done offline after the data collection phase. To implement the eDDPC scheme, the following finite-horizon optimal control problem is solved at each time t

$$\min_{\beta(t), \bar{w}(t)} \sum_{k=0}^{L-1} l(\bar{w}_k(t)) \quad (7a)$$

$$\text{s.t. } \bar{w}_{[-n, L-1]}(t) = P\beta(t) \quad (7b)$$

$$\bar{w}_{[-n, -1]}(t) = w_{[t-n, t-1]}^{\text{on}} \quad (7c)$$

$$\bar{w}_{[L-n, L-1]}(t) = w_n^s \quad (7d)$$

$$\bar{w}_k(t) \in \mathbb{W}, \quad \forall k \in \mathbb{Z}_{[0, L-1]}. \quad (7e)$$

Here, $\bar{w}(t) \in \mathbb{R}^{q(L+n)}$ refers to the predicted input-output trajectories at time t , while online measurements are denoted by w_t^{on} . The stage cost (7a) is a quadratic function that penalizes the deviation from the given set point, i.e., $l(\bar{w}_k(t)) = \|\bar{w}_k(t) - w^s\|_W^2$, for some $W \succ 0$. Finally, \mathbb{W} denotes the constraint set and is defined as

$$\mathbb{W} := \{w = \begin{bmatrix} u \\ y \end{bmatrix} \mid u \in \mathbb{U} \subseteq \mathbb{R}^m, y \in \mathbb{Y} \subseteq \mathbb{R}^p\}, \quad (8)$$

where \mathbb{U}, \mathbb{Y} are input and output constraint sets, respectively, with $w^s \in \text{int}(\mathbb{W})$. Once a solution to (7) is found (denoted $\beta^*(t)$ and $\bar{w}^*(t)$), the first instant of the optimal input $\bar{u}^*(t)$ is applied to the system and the process is repeated in a receding horizon fashion (see Algorithm 2).

Notice that, since $\text{im}(P) = \text{im}(\mathcal{H}_{L+n}(w))$, it follows that eDDPC (7) and existing DDPC schemes that rely on the use of Hankel matrices are equivalent and the resulting closed-loop trajectories of the corresponding schemes are identical (see [27] for details). Another implication of the equivalence of these schemes is that the proposed eDDPC scheme retains the same theoretical guarantees as the ones shown in [8] for the nominal case.

² The length of the predicted trajectories is extended by n instances to account for fixing the initial conditions (cf. (7c)).

Algorithm 2. Nominal eDDPC scheme

Input: Measurements $w \in \mathcal{B}|_T$, where $\mathcal{B} \in \partial \mathcal{L}_{m,n,\ell}^q$, satisfying $\text{rank}(\mathcal{H}_d(w)) = md + n$ for $d \geq \ell + 1$.

Offline phase: run Algorithm 1 to obtain P .

Online phase:

1. At time t , use measurements $w_{[t-n, t-1]}^{\text{on}}$ to solve (7).
 2. Apply the input $u_t = \bar{u}_0^*(t)$ to the system.
 3. Set $t = t + 1$ and return to Step 1.
-

In the following, we consider noisy output measurements (both in the offline and online phases) and later propose a robust eDDPC scheme. To show recursive feasibility and practical stability of the resulting closed-loop system, we first provide in the next section a novel result on uncertainty quantification in the behavioral framework.

4 Uncertainty quantification in the behavioral framework

We now consider output³ measurements which are affected by uniformly bounded measurement noise. In particular, one has access to measurements \tilde{w} , whose elements take the form

$$\tilde{w}_k = \begin{bmatrix} u_k \\ \tilde{y}_k \end{bmatrix} = \begin{bmatrix} u_k \\ y_k \end{bmatrix} + \begin{bmatrix} 0 \\ \epsilon_k \end{bmatrix} =: w_k + \epsilon_k, \quad (9)$$

where $\|\epsilon_k\|_\infty = \|\epsilon_k\|_\infty \leq \bar{\epsilon}$ for all $k \geq 0$. When applying a persistently exciting input to the system and collecting noisy output data, the corresponding data matrix, in general, satisfies $\text{rank}(\mathcal{H}_d(\tilde{w})) \geq md + n$. A possible remedy is to first obtain a low rank approximation $\widehat{\mathcal{H}}$ of $\mathcal{H}_d(\tilde{w})$ such that $\text{rank}(\widehat{\mathcal{H}}) = md + n$. Low rank approximation can be done using, e.g., truncated singular-value decomposition (TSVD, cf. [31]), or using structured low-rank approximation of Hankel matrices (SLRA, cf. [32]).

To illustrate the use of TSVD, let the singular value decomposition of $\mathcal{H}_d(\tilde{w})$ be given by

$$\mathcal{H}_d(\tilde{w}) = \begin{bmatrix} U & W \end{bmatrix} \text{diag}(S_1, S_2) \begin{bmatrix} V & Q \end{bmatrix}^\top, \quad (10)$$

where $S_1 = \text{diag}(s_1(\mathcal{H}_d(\tilde{w})), \dots, s_{md+n}(\mathcal{H}_d(\tilde{w})))$, while S_2 is a rectangular diagonal matrix that contains the remaining singular values. Furthermore, U, W, V, Q are semi-orthonormal matrices of appropriate dimensions.

An approximate matrix $\widehat{\mathcal{H}}$ can now be obtained as

$$\widehat{\mathcal{H}} = US_1V^\top. \quad (11)$$

³ Our analysis is also applicable for the case when noise affects both input and output channels. Here, we focus on output noise since this is the standard setting considered in DDPC literature (see, e.g., [8, 9]).

Since $\text{rank}(\widehat{\mathcal{H}}) = md + n$ (by construction), we can now follow the steps in Algorithm 1 to obtain a matrix \widehat{P} whose image defines an approximation of the finite-length behavior of the system, i.e., $\text{im}(\widehat{P}) =: \widehat{\mathcal{B}}|_{L+n}$. In Section 5.1, we will use \widehat{P} as a predictor in a robust eDDPC scheme. To later prove stability of such a scheme, we first need to quantify the discrepancy between the (unknown) true behavior $\mathcal{B}|_{L+n} = \text{im}(P)$ and the (known) approximate behavior $\widehat{\mathcal{B}}|_{L+n} = \text{im}(\widehat{P})$.

Discrepancy between behaviors is typically studied in terms of the *distance* between them [33]. The recent works [29, 30] define new metrics between (known) behaviors along with methods to compute them. However, the results there cannot be readily used in our setting, since the true behavior is unknown in our case and, therefore, a bound on the distance measure must be derived instead. To this end, we provide a novel result on uncertainty quantification in the behavioral framework. In particular, since $\mathcal{B}|_{L+n}$ and $\widehat{\mathcal{B}}|_{L+n}$ are subspaces (of the same dimension), we consider the *angles* between them as a distance measure and provide bounds on the angles in terms of the noise level $\bar{\varepsilon}$. To achieve this, we rely on results from SVD perturbations [28].

4.1 SVD perturbations

Consider a matrix $M \in \mathbb{R}^{m \times n}$ with $m \leq n$ and let its perturbation be $\widehat{M} = M + E$ with $\|E\|_F < \infty$, such that $0 < r = \text{rank}(M) \leq \rho = \text{rank}(\widehat{M}) \leq m$. We consider a decomposition of M and \widehat{M} of the following form

$$\begin{aligned} M &= \begin{bmatrix} U_M & W_M \end{bmatrix} \text{diag}(S_M, 0) \begin{bmatrix} V_M & Q_M \end{bmatrix}^\top, \\ \widehat{M} &= \begin{bmatrix} U_{\widehat{M}} & W_{\widehat{M}} \end{bmatrix} \text{diag}(S_{1,\widehat{M}}, S_{2,\widehat{M}}) \begin{bmatrix} V_{\widehat{M}} & Q_{\widehat{M}} \end{bmatrix}^\top, \end{aligned} \quad (12)$$

where $S_M = \text{diag}(s_1(M), \dots, s_r(M))$ (similarly for $S_{1,\widehat{M}}$), whereas $S_{2,\widehat{M}}$ contains the remaining singular values. The matrices U_M, W_M and V_M, Q_M (similarly for $U_{\widehat{M}}, W_{\widehat{M}}, V_{\widehat{M}}, Q_{\widehat{M}}$) are semi-orthonormal matrices of appropriate dimensions whose columns represent the right and left singular vectors, respectively. The image of these matrices are known as the *singular subspaces*. We are interested in quantifying the effect of the disturbance E on the decomposition of M and \widehat{M} . The following theorem states that the singular values of perturbed matrix \widehat{M} remain in a neighborhood around the corresponding singular values of M .

Theorem 6 [28] *Given $M, \widehat{M} = M + E \in \mathbb{R}^{m \times n}$ where $0 < r = \text{rank}(M) \leq \rho = \text{rank}(\widehat{M}) \leq m$ and $\|E\|_F < \infty$, let their SVDs be given by (12). Then,*

$$\sqrt{\sum_{i=1}^{\rho} (s_i(\widehat{M}) - s_i(M))^2} \leq \|E\|_F. \quad (13)$$

A similar result cannot, in general, be provided for the singular vectors (cf. [28, Sec. 6]). This is because singular vectors form a basis for the singular subspaces and, hence, are not unique. A more suitable measure is provided by the *principal angles* between the true and perturbed singular subspaces, which are defined as follows.

Definition 3 [34] *Let \mathcal{X}, \mathcal{Y} be two subspaces of \mathbb{R}^n of dimension $k \leq n$. The principal angles $\theta_i, 0 \leq \theta_i \leq \pi/2$ for $i \in \mathbb{Z}_{[1,k]}$, between \mathcal{X}, \mathcal{Y} are recursively defined by*

$$\begin{aligned} \cos \theta_i &= \bar{x}_i^\top \bar{y}_i = \arg \max_{x_i \in \mathcal{X}} \max_{y_i \in \mathcal{Y}} x_i^\top y_i \\ \text{s.t. } &\|x_i\|_2 = \|y_i\|_2 = 1, \\ &x_i^\top \bar{x}_j = 0, y_i^\top \bar{y}_j = 0, \forall j \in \mathbb{Z}_{[1,i-1]}, \end{aligned} \quad (14)$$

where $\bar{x}_i, \bar{y}_i \in \mathbb{R}^n, i \in \mathbb{Z}_{[1,k]}$, are principal vectors which form orthonormal bases for \mathcal{X}, \mathcal{Y} , respectively.

Principal vectors always exist and, although the vectors are not unique, the principal angles are unique. For the remainder of the paper, we define the matrix of principal angles between \mathcal{X}, \mathcal{Y} as $\Theta(\mathcal{X}, \mathcal{Y}) = \text{diag}(\theta_1, \dots, \theta_k)$.

The following theorem states that the angle between the true and perturbed singular subspaces can be bounded in terms of $\|E\|_F$. Here, we recall the result only in terms of $\Theta(\text{im}(U_M), \text{im}(U_{\widehat{M}}))$ for notational simplicity, however the same bound holds for all other singular subspaces.

Theorem 7 [28] *Consider $M, \widehat{M} = M + E \in \mathbb{R}^{m \times n}$ where $0 < r = \text{rank}(M) \leq \rho = \text{rank}(\widehat{M}) \leq m$ and $\|E\|_F < \infty$, along with their decomposition (12). Then,*

$$\|\sin(\Theta(\text{im}(U_M), \text{im}(U_{\widehat{M}})))\|_F \leq \frac{\sqrt{2}}{\delta} \|E\|_F. \quad (15)$$

where $\delta = s_r(\widehat{M})$, and $\sin(\cdot)$ is applied element-wise.

Theorem 7 provides a perturbation bound on the angles between two singular subspaces in terms of the perturbation E . Notice that δ corresponds to the r -th singular value of \widehat{M} (which is strictly positive since $\text{rank}(\widehat{M}) = \rho \geq \text{rank}(M) = r > 0$). As a result, the value of $\delta = s_r(\widehat{M})$ is also affected by E . As a consequence of Theorem 6, it holds that

$$\begin{aligned} -\|E\|_F &\leq s_r(\widehat{M}) - s_r(M) \leq \|E\|_F \\ \implies s_r(M) - \|E\|_F &\leq \delta \leq s_r(M) + \|E\|_F. \end{aligned} \quad (16)$$

This can now be used to further bound (15) as follows

$$\|\sin(\Theta(\text{im}(U_M), \text{im}(U_{\widehat{M}})))\|_F \leq \frac{\sqrt{2}}{s_r(M) - \|E\|_F} \|E\|_F,$$

which is well defined if $s_r(M) > \|E\|_F$. Notice that the right hand side goes to zero as $\|E\|_F$ goes to zero.

Before Definition 3, we pointed out that the difference between singular vectors, e.g., $\|U_M - U_{\widehat{M}}\|_F$, cannot in general be bounded by the norm of $\|E\|_F$. This is because singular vectors form a basis for the corresponding singular subspaces and, hence, are not unique. The following lemma exploits the non-uniqueness property of the singular vectors and shows that if a basis for one singular subspace (e.g., $\text{im}(U_{\widehat{M}})$ in Theorem 7) is fixed, then one can always find a basis for the other subspace (e.g., $\text{im}(U_M)$) such that their difference is bounded by the angles between the two subspaces and, hence, also bounded by $\|E\|_F$ as in Theorem 7. This is an important result which will later be used in Theorem 9.

Lemma 8 Consider $M, \widehat{M} = M + E \in \mathbb{R}^{m \times n}$ where $0 < r = \text{rank}(M) \leq \rho = \text{rank}(\widehat{M}) \leq m$ and $\|E\|_F < \infty$, along with their decomposition (12). Then, there exists \widetilde{U}_M such that $\text{im}(\widetilde{U}_M) = \text{im}(U_M)$ and

$$\|U_{\widehat{M}} - \widetilde{U}_M\|_F \leq 2\sqrt{r}\|\sin(\Theta(\text{im}(U_M), \text{im}(U_{\widehat{M}})))\|_F, \quad (17)$$

where $\delta = s_r(\widehat{M})$, and $\sin(\cdot)$ is applied element-wise.

PROOF. See Appendix A.

It is important to explain the usefulness of Lemma 8. Specifically, it allows us to bound the difference between a (known) basis of one singular subspace with respect to some other (potentially unknown) basis of the perturbed subspace, in terms of the angles between the two subspaces and, consequently, in terms of $\|E\|_F$. This is important since, in the context of data-based representations, one typically has access to matrices of noisy data, whose associated subspaces of their low-rank approximations correspond to a known estimate of the true restricted behavior of the system, while the true noise-free data matrix (and, hence, the true behavior) is unknown. In the following subsection, we exploit the previous perturbation bounds to quantify the difference between the true and estimated behaviors $\mathcal{B}|_{L+n}$ and $\widehat{\mathcal{B}}|_{L+n}$, respectively, which is the main result of this section.

4.2 Uncertainty quantification

In this section, we are interested in quantifying the discrepancy between $\mathcal{B}|_{L+n}$ and $\widehat{\mathcal{B}}|_{L+n}$. By definition, these subspaces are given by $\text{im}(P)$ and $\text{im}(\widehat{P})$, where $P = \text{null}(\Gamma)$ and $\widehat{P} = \text{null}(\widehat{\Gamma})$. The matrices Γ and $\widehat{\Gamma}$ are given by $(L+n-d)$ shifts of R_d and \widehat{R}_d as in (6), respectively, where the rows of R_d and \widehat{R}_d define a basis for the left null spaces of $\mathcal{H}_d(w)$ and $\widehat{\mathcal{H}}$, respectively. Recall that the latter matrix, i.e., $\widehat{\mathcal{H}}$, was obtained following a TSVD approximation of $\mathcal{H}_d(\widehat{w})$ (cf. (11)). The following theorem is the main result of this section. It provides a bound on the angle between the true and estimated restricted behaviors of the system in terms of the bound on the noise in the available data.

Theorem 9 Given noisy measurements \widehat{w} of a trajectory $w \in \mathcal{B}|_T$ as in (9) where $\|\varepsilon_k\|_\infty \leq \bar{\varepsilon}$ and $\mathcal{B} \in \partial \mathcal{L}_{m,n,\ell}^q$, let $\text{rank}(\mathcal{H}_d(\widehat{w})) \geq \text{rank}(\mathcal{H}_d(w)) = md+n$. For any $L \geq d \geq \ell + 1$, let $\widehat{\mathcal{B}}|_{L+n} := \text{im}(\widehat{P})$ where \widehat{P} is obtained by Algorithm 1 following a TSVD approximation of $\mathcal{H}_d(\widehat{w})$. Then,

$$\|\sin \Theta(\widehat{\mathcal{B}}|_{L+n}, \mathcal{B}|_{L+n})\|_F \leq \frac{C_\theta}{\delta_1 \delta_2} \bar{\varepsilon}, \quad (18)$$

where $C_\theta = 8\sqrt{qd(L+n-d+1)(md+n)(T-d+1)}$, $\delta_1 = s_{p(L+n)-n}(\widehat{\Gamma})$, $\delta_2 = s_{md+n}(\widehat{\mathcal{H}})$ and $\sin(\cdot)$ is applied element-wise.

PROOF. See Appendix B.

Theorem 9 provides a perturbation bound on the angles between the true (unknown) finite-length behavior and its known estimate from noisy data, in terms of the noise level. In contrast, existing results on uncertainty quantification in the behavioral framework [29, 30] provide computational methods to compute the distance/angle between two *known* behaviors.

Notice that larger values of δ_1, δ_2 lead to tighter error bounds. Here, $\delta_2 = s_{md+n}(\widehat{\mathcal{H}})$ which, due to TSVD, is also equal to $s_{md+n}(\mathcal{H}_d(\widehat{w}))$. It was shown in [35, Th. 6] that a lower bound on $s_{md+n}(\mathcal{H}_d(\widehat{w}))$ can be guaranteed by suitable design of the input. Simply put, inputs with larger *quantitative levels of PE* result in large values of δ_2 , thus reducing the bound in (18) and, hence, the estimated behavior gets closer to the true behavior.

Similar to the discussion following Theorem 7, the bound in (18) can also be shown to go to zero as $\bar{\varepsilon} \rightarrow 0$. To see this, notice that δ_1 can be bounded similarly to (16) as $s_{p(L+n)-n}(\Gamma) - \|\widehat{\Gamma} - \Gamma\|_F \leq \delta_1$. Using (B.5), (B.15) (see Appendix B) and some standard manipulations, the following inequality is obtained

$$\frac{1}{\delta_1} \leq \frac{\delta_2}{\delta_2 s_{p(L+n)-n}(\Gamma) - \rho_1 \bar{\varepsilon}}, \quad (19)$$

where $\rho_1 := 4c_1 \sqrt{2qd(md+n)(T-d+1)}$. Plugging this back into (18) results in

$$\|\sin \Theta(\widehat{\mathcal{B}}|_{L+n}, \mathcal{B}|_{L+n})\|_F \leq \frac{C_\theta / s_{p(L+n)-n}(\Gamma)}{\delta_2 - \bar{\rho}_1 \bar{\varepsilon}} \bar{\varepsilon}, \quad (20)$$

where $\bar{\rho}_1 = \rho_1 / s_{p(L+n)-n}(\Gamma)$. Using (B.13) and following similar steps that led to (19), we obtain

$$\frac{1}{\delta_2 - \bar{\rho}_1 \bar{\varepsilon}} \leq \frac{1}{s_{md+n}(\mathcal{H}_d(w)) - (\bar{\rho}_1 + \rho_2) \bar{\varepsilon}}, \quad (21)$$

for $\rho_2 := 2\sqrt{qd(T-d+1)}$. Finally, we can further

bound (20) using (21) as follows

$$\begin{aligned} & \|\sin \Theta(\widehat{\mathcal{B}}|_{L+n}, \mathcal{B}|_{L+n})\|_F \\ & \leq \frac{C_\theta / s_{p(L+n)-n}(\Gamma)}{s_{md+n}(\mathcal{H}_d(w)) - (\bar{\rho}_1 + \rho_2)\bar{\varepsilon}} \bar{\varepsilon}. \end{aligned} \quad (22)$$

From here, it is easy to see that the bound goes to zero as $\bar{\varepsilon} \rightarrow 0$, provided that $s_{md+n}(\mathcal{H}_d(w)) > (\bar{\rho}_1 + \rho_2)\bar{\varepsilon}$, where $s_{md+n}(\mathcal{H}_d(w))$ is the smallest non-zero singular value of the noise-free Hankel matrix. Such a condition can be guaranteed by design of input (cf. [35, Th. 4]).

Remark 10 *For simplicity, the results of Theorem 9 assume that the offline data is consecutive. However, a qualitatively similar bound to (18) can be obtained for the case of irregularly measured data, provided that one can compute \widehat{R}_d from the available data (cf. [26, Alg. 3]).*

Remark 11 *The results of Theorem 9 are cast in terms of the matrix \widehat{P} . A similar bound can be also derived if one directly works with the Hankel matrices of data. This, however, requires the availability of longer sequences of PE input-output data which is not the setting considered in this paper. Such a bound can be used to provide stability analysis for, e.g., the robust DDPC scheme from [25], but is potentially of interest in applications beyond DDPC.*

By combining the results of Lemma 8 and Theorem 9 together with (22), we obtain the following corollary.

Corollary 12 *Let the assumptions of Theorem 9 hold and suppose that $s_{md+n}(\mathcal{H}_d(w)) > (\bar{\rho}_1 + \rho_2)\bar{\varepsilon}$. Then, there exists P such that $\text{im}(P) = \mathcal{B}|_{L+n}$ and*

$$\|\widehat{P} - P\|_F \leq \frac{2\sqrt{m(L+n)} + nC_\theta / s_{p(L+n)-n}(\Gamma)}{s_{md+n}(\mathcal{H}_d(w)) - (\bar{\rho}_1 + \rho_2)\bar{\varepsilon}} \bar{\varepsilon}, \quad (23)$$

where $C_\theta, \delta_1, \delta_2$ are as in (18) and $\bar{\rho}_1, \rho_2$ are as in (22).

In the following section, we propose a robust version of the efficient data-driven predictive control scheme in (7) and use (23) to later prove recursive feasibility and practical stability of the resulting scheme.

5 Robust eDDPC

As explained in the previous sections, the image of \widehat{P} defines an approximation of the finite-length behavior of the system. If such a matrix is used in the eDDPC scheme (7) in place of P , the problem might be infeasible since the predicted sequences $\widehat{w}(t)$ are no longer guaranteed to be trajectories of the system. This necessitates certain modifications for the eDDPC scheme to account for measurement noise (in both the online and offline phases). In this section, we propose a robust formulation of the eDDPC scheme, then compare its sample and computational requirements against existing schemes from

Algorithm 3. Robust eDDPC scheme

Input: Measurements \widehat{w} of $w \in \mathcal{B}|_T$, where $\mathcal{B} \in \partial \mathcal{L}_{m,n,\ell}^q$, satisfying $\text{rank}(\mathcal{H}_d(\widehat{w})) \geq md+n$ for $d \geq \ell+1$.

Offline phase: Obtain a low-rank approximation $\widehat{\mathcal{H}}$ of $\mathcal{H}_d(\widehat{w})$ such that $\text{rank}(\widehat{\mathcal{H}}) = md+n$, and follow Algorithm 1 to obtain \widehat{P} .

Online phase:

1. At time t , use measurements $\widehat{w}_{[t-n,t-1]}^{\text{on}}$ to solve (24).
 2. Apply the input $u_{[t,t+n-1]} = \widehat{u}_{[0,n-1]}^*(t)$ to the system.
 3. Set $t = t+n$ and return to Step 1.
-

the literature. Later, we prove recursive feasibility and practical stability of the closed-loop system. To that end, we use the results of Corollary 12 and follow the proof technique presented in [9], which lays a framework to analyze robustness of DDPC schemes based on inherent robustness of nominal MPC schemes [1, Sec. 3.5].

5.1 Robust scheme

In this subsection, we propose a robust formulation of the eDDPC scheme which uses \widehat{P} as a predictor. Specifically, at time t we use the most recent online noisy measurements $\{\widehat{w}_k^{\text{on}}\}_{k=t-n}^{t-1}$ to solve the following finite-horizon optimal control problem

$$\min_{\widehat{\beta}(t), \widehat{w}(t), \widehat{\sigma}(t)} \sum_{k=0}^{L-1} l(\widehat{w}_k(t)) + \lambda_\beta \bar{\varepsilon}^{\mu_\beta} \|\widehat{\beta}(t)\|_2^2 + \frac{\lambda_\sigma}{\bar{\varepsilon}^{\mu_\sigma}} \|\widehat{\sigma}(t)\|_2^2 \quad (24a)$$

$$\text{s.t. } \widehat{w}_{[-n,L-1]}(t) + \widehat{\sigma}(t) = \widehat{P}\widehat{\beta}(t) \quad (24b)$$

$$\widehat{w}_{[-n,-1]}(t) = \widehat{w}_{[t-n,t-1]}^{\text{on}} \quad (24c)$$

$$\widehat{w}_{[L-n,L-1]}(t) = w^s \quad (24d)$$

$$\widehat{w}_k(t) \in \mathbb{W}, \quad \forall k \in \mathbb{Z}_{[0,L-1]}. \quad (24e)$$

To mitigate the effect of noise (both in the online and offline phases), we include a slack variable $\widehat{\sigma}(t) \in \mathbb{R}^{q(L+n)}$ and regularize it in the cost function along with the regressor vector $\widehat{\beta}(t)$ using regularization parameters $\lambda_\beta, \lambda_\sigma, \mu_\beta, \mu_\sigma > 0$. Such regularization techniques are standard in existing works on robust DDPC (cf., [9, 19, 36] and many others [23]). Here, we use $\widehat{w}(t), \widehat{\beta}(t), \widehat{\sigma}(t)$ to denote the decision variables of the robust scheme, to distinguish it from $\bar{w}(t), \beta(t)$ that were used for the nominal scheme (7). The optimal solutions of (24) at time t are denoted by $\widehat{w}^*(t), \widehat{\beta}^*(t), \widehat{\sigma}^*(t)$.

Unlike (7), here we use a multi-step (specifically, n step) receding horizon scheme. In particular, once a solution for (24) is found, we apply the first n instances of the optimal input $\widehat{u}^*(t)$. Afterwards, the horizon is shifted by n steps and the procedure is repeated (see Algorithm 3). In the following subsection, we discuss the sample and computational efficiency of our proposed robust scheme.

Table 1

Analytic comparison between eDDPC and existing DDPC schemes.

Note that for sDDPC each segment is at least $T_{\text{seg}} \geq \ell$, and for eDDPC d satisfies $d \geq \ell + 1$.

| | DDPC [8] | sDDPC [24] | SVD-DDPC [25] | eDDPC |
|----------------|-----------------|---------------------------------------|-----------------|----------------|
| $T \geq$ | $(m+1)(L+2n)-1$ | $(m+1)(2T_{\text{seg}}+n)-1$ | $(m+1)(L+2n)-1$ | $(m+1)(d+n)-1$ |
| dim(regressor) | $T-L-n+1$ | $n_{\text{seg}}(T-2T_{\text{seg}}+1)$ | $m(L+n)+n$ | $m(L+n)+n$ |

5.2 Sample and computational efficiency

In this section, we analytically compare the sample and computational requirements of our proposed robust eDDPC scheme (24) to (i) the DDPC scheme of [8], (ii) the segmented DDPC (sDDPC) scheme of [24] and (iii) the SVD-based DDPC scheme (SVD-DDPC) of [25]. Here, sample requirements refer to the minimum number of offline data points required for successful application of the DDPC schemes, whereas computational requirements are expressed in terms of the dimension of the regressor vector (e.g., $\hat{\beta}(t)$ in (24)).

Recall that (24) uses \hat{P} as a predictor, which can be obtained from short and noisy data. In particular, given \tilde{w} one can construct $\mathcal{H}_d(\tilde{w})$ for $d \geq \ell + 1$, and obtain a low-rank approximation of it (e.g., by TSVD as in (11) or by SLRA), then follow the steps in Algorithm 1 to arrive at \hat{P} . One can ensure that $\text{rank}(\mathcal{H}_d(\tilde{w})) \geq md + n$ by applying a PE input of order $d + n$ (cf. Theorem 1), which necessitates that the offline data must be at least $T \geq (m+1)(d+n)-1$ long, independent of the prediction horizon length L . In contrast, both DDPC and SVD-DDPC schemes [8, 25] require at least $T \geq (m+1)(L+n)-1$ samples. For sDDPC [24], the length of each segment must satisfy $T_{\text{seg}} \geq \ell$. Assuming that the prediction horizon is an integer multiple of T_{seg} (i.e., $L = n_{\text{seg}}T_{\text{seg}}$ where n_{seg} is the number of segments), sDDPC and eDDPC schemes would use the same number of data points only when $T_{\text{seg}} = \ell = 1$. Otherwise, eDDPC always uses less data points. Finally, we emphasize that, unlike other schemes, the robust eDDPC scheme (24) can be applied when the offline data contains irregularly measured samples, provided that \hat{R}_d can be computed from the available samples (see [26, Alg. 3]). Table 1 summarizes this comparison and highlights the fact that robust eDDPC is the most sample-efficient DDPC scheme.

Table 1 also lists the dimension of the regressor vector in the optimal control problem of each scheme. Compared to sDDPC, eDDPC always has a smaller regressor vector, which is equal to that of SVD-DDPC. In contrast, the size of DDPC's regressor grows as more offline data is used. Notice that in the nominal setting, eDDPC is the most sample and computationally efficient scheme (cf. the preliminary conference version [27] for a detailed comparison in the nominal setting).

In the robust setting, however, the regressor vector is

not the only decision variable in the optimization problems, but also the slack variables (e.g., $\hat{\sigma}(t)$ in (24)). In [8], the robust DDPC scheme uses $p(L+n)$ slack variables to account for noise in the output. Even when considering only output noise in our setting, the robust eDDPC scheme in (24) uses $q(L+n)$ slack variables (where $q = m+p$). The increased number of the slack variables is due to the pre-processing steps performed when building the matrix \hat{P} . Specifically, when low-rank approximation is performed on the noisy data matrix $\mathcal{H}_d(\tilde{w})$ (cf. (11)), all the entries of the resulting approximate matrix $\hat{\mathcal{H}}$ (and, subsequently \hat{P}) are potentially affected by the output measurement noise. As a result, more slack variables are needed⁴ when later showing stability and recursive feasibility of the robust eDDPC scheme (see Section 5.3). The sDDPC and SVD-DDPC schemes of [24, 25] only consider slack variables to enhance closed-loop performance but do not provide any closed-loop guarantees (recursive feasibility and robust stability) in case of noisy data. The above discussion illustrates that an accurate comparison of the computational efficiency depends on the desired characteristics (e.g., stability guarantees) of the scheme at hand.

5.3 Stability guarantees

In this subsection, we show that the robust eDDPC scheme (24) is recursively feasible and that the resulting closed-loop system is practically stable.

Remark 13 Here, we use TSVD to later obtain \hat{P} as explained above. This enables us to use the uncertainty quantification result in Corollary 12. Alternatively one can use SLRA [32] to obtain $\hat{\mathcal{H}}$ and later follow Algorithm 1 to obtain \hat{P} . We expect that similar stability and recursive feasibility guarantees hold for an SLRA-based eDDPC scheme. Section 6 illustrates that SLRA-eDDPC results in a better closed-loop performance than TSVD-eDDPC. This might be attributed to the fact that SLRA returns a better approximation of (and of the same structure as) the noise-free matrix compared to TSVD.

For simplicity, we consider here the problem of stabilizing the origin, i.e., $w^s = 0$, although non-zero setpoints can be considered with slight modifications of the following proofs. Unlike the nominal case, we consider the

⁴ In our simulations, we observed that when using only $p(L+n)$ slack variables, nearly identical performance is achieved while improving the computational efficiency.

following assumptions on the constraint set \mathbb{W} (see (8)).

Assumption 1 *The set \mathbb{U} is a convex compact polytope and $\mathbb{Y} = \mathbb{R}^p$.*

Output constraints are not considered here for brevity. Methods to address output constraint satisfaction in robust DDPC can be found in, e.g., [37]. Similar to [9], we make the following additional assumption.

Assumption 2 *Problem (24) satisfies the linear independence constraint qualification (LICQ). Furthermore, we assume that $\mu_\beta + \mu_\sigma < 2$.*

The LICQ assumption corresponds to requiring that the row entries of the equality and active inequality constraints are linearly independent. Moreover, the requirement $\mu_\beta + \mu_\sigma < 2$ can be satisfied by design of the regularization parameters and is required for the following proofs. Since only input-output data is available, we define the non-minimal state $\xi_t = \Pi w_{[t-n, t-1]} = [u_{[t-n, t-1]}^\top y_{[t-n, t-1]}^\top]^\top$ for some suitable permutation matrix Π (similarly, $\tilde{\xi}_t$ denotes the noisy extended state, cf. (9)). The state-space representation corresponding to ξ is detectable [38]. Hence, there exists an input-output-to-state stability (IOSS) Lyapunov function $V_{\text{IOSS}}(\xi) = \|\xi\|_X^2$ satisfying

$$V_{\text{IOSS}}(\xi_{t+1}) - V_{\text{IOSS}}(\xi_t) \leq -\frac{1}{2}\|\xi_t\|^2 + c\|w_t\|^2, \quad (25)$$

for some $X > 0$ and $c > 0$ [39]. Using V_{IOSS} , we define

$$V(\xi_t) = J_L^*(\xi_t) + \frac{1}{c}V_{\text{IOSS}}(\xi_t), \quad (26)$$

where $J_L^*(\xi_t)$ denotes the optimal cost of (7). As in [9], we assume that it is quadratically bounded, which is, e.g., satisfied in case of polytopic constraints [40].

Assumption 3 *There exists $c_J > 0$ such that $J_L^*(\xi) \leq c_J\|\xi\|_2^2$ for any ξ such that Problem (7) is feasible.*

The function $V(\xi_t)$ in (26) can now be used (i) to show exponential stability of the nominal scheme (7) and (ii) as a practical Lyapunov function [41, Def. 2.3] for the robust eDDPC scheme (24) in the presence of noise.

As mentioned earlier, we will proceed to prove recursive feasibility and practical stability following the framework laid in [9]. Specifically, the effect of output measurement noise is first translated into an input disturbance of a nominal scheme. Then, by exploiting the inherent robustness of the nominal scheme, one can eventually show practical stability of the eDDPC scheme in (24). This is summarized in the following theorem.

Theorem 14 *Given noisy measurements \tilde{w} of a trajectory $w \in \mathcal{B}|_T$ where $\mathcal{B} \in \partial\mathcal{L}_{m,n,\ell}^q$ is controllable, let*

$u \in (\mathbb{R}^m)^T$ be PE of order $d+n$ for $d \geq \ell+1$. Further, let Assumptions 1-3 and the assumptions of Corollary 12 hold, and let \mathcal{B} be controlled by an n -step eDDPC scheme based on (24) for $L \geq \max\{2n, d\}$. Then, for any $\bar{V} > 0$, there exist $\varepsilon^, c_{V_1}, c_{V_2} > 0$, $c_{V_3} \in (0, 1)$ and $\phi \in \mathcal{K}_\infty$ such that, for all initial conditions ξ_0 satisfying $V(\xi_0) \leq \bar{V}$ and all $\bar{\varepsilon} \leq \varepsilon^*$, Problem (24) is feasible for $t = in$, $i \in \mathbb{N}$, and the closed-loop system satisfies*

$$c_{V_1}\|\xi_t\|_2^2 \leq V(\xi_t) \leq c_{V_2}\|\xi_t\|_2^2, \quad (27)$$

$$V(\xi_{t+n}) \leq c_{V_3}V(\xi_t) + \phi(\varepsilon^*). \quad (28)$$

PROOF. See Appendix C. The proof follows similar steps as the proofs of [9, Th. IV.1, Prop. IV.1 and Cor. IV.1] and consists of the following main steps: (i) Translating the measurement noise to an input disturbance for a nominal DDPC scheme. (ii) Showing that the multi-step nominal scheme is inherently robust with respect to input-disturbances and, (iii) establishing practical stability of the robust DDPC scheme (24). The important difference of our setting compared to [9] is the use of \hat{P} as a predictor in (24) and, therefore, the proof requires several modifications which crucially depend on the uncertainty quantification result of Corollary 12.

Theorem 14 shows that if the n -step robust eDDPC scheme is initially feasible, then it is recursively feasible and the closed-loop system is practically (exponentially) stable. Specifically, the closed-loop trajectories converge to a region \mathbb{V} around the origin whose size is proportional to the noise level. As in [9], this result is qualitative and quantifying \mathbb{V} without model knowledge can be difficult.

The results of Theorem 14 can potentially be more conservative than the analogous ones presented in [9] for a robust DDPC scheme that uses Hankel matrices of noisy data. This is because our analysis uses the uncertainty quantification result in Theorem 9, for which the corresponding bounds tend to be conservative. In contrast, the uncertainty due to additive noise in [9] can easily be separated and upper bounded (due to the use of Hankel matrices). However, as explained below Remark 10, larger quantitative orders of PE lead to tighter error bounds in (23). An important advantage of the robust eDDPC over the robust scheme from [9] is that it achieves practically comparable performance with very little number of data points, for which the robust scheme from [9] cannot even be implemented, as shown in the following section.

6 Simulations

In this section, we consider the problem of regulating a (known) non-zero set point of the (linearized) four tank system. We shall compare the performance of the eDDPC scheme (24) against the DDPC and SVD-DDPC

schemes from [9, 25], respectively, for different numbers of available noisy offline data points. In the case of eDDPC, we also compare the use of two different low-rank approximation methods in Algorithm 3. When TSVD is used, we refer to the scheme as eDDPC, and when SLRA is used we refer to it as SLRA-eDDPC.

The linearized state space model of the four tank system is given by (see [8])

$$\begin{aligned} x_{k+1} &= \begin{bmatrix} 0.921 & 0 & 0.041 & 0 \\ 0 & 0.918 & 0 & 0.033 \\ 0 & 0 & 0.924 & 0 \\ 0 & 0 & 0 & 0.937 \end{bmatrix} x_k + \begin{bmatrix} 0.017 & 0.001 \\ 0.001 & 0.023 \\ 0 & 0.061 \\ 0.072 & 0 \end{bmatrix} u_k \\ y_k &= \begin{bmatrix} 1 & 0 & 0 & 0 \\ 0 & 1 & 0 & 0 \end{bmatrix} x_k + \varepsilon_k, \end{aligned} \quad (29)$$

where $x_k \in \mathbb{R}^4$, $u_k, y_k, \varepsilon_k \in \mathbb{R}^2$ are the state, input, output and measurement noise at time step k , respectively. The objective is to use the above DDPC schemes to stabilize the set point $w^s = [(u^s)^\top (y^s)^\top]^\top$ with $(u^s)^\top = [1 \ 1]$ and $(y^s)^\top = [0.65 \ 0.77]$. For all schemes, we use a prediction horizon $L = 16$ and impose the following input constraints $\mathbb{U} = [-2, 2]^2$. Furthermore, we use a quadratic stage cost $l(\bar{w}_k(t)) = \|\bar{w}_k(t) - w^s\|_W^2$ with $W = \text{diag}(10^{-2}I_2, 3I_2)$.

To collect the offline data, we perform an open-loop simulation by applying a random input and introducing noise sampled from uniform random distributions: $u_k \sim U(-4, 4)^2$ and $\varepsilon_k \sim U(-4 \cdot 10^{-3}, 4 \cdot 10^{-3})^2$, respectively. Several such simulations are performed in order to collect data of different lengths⁵ $T \in \{23, 35, 47, 59, 71, 100, 200, 300\}$. This is because, unlike DDPC and SVD-DDPC, our proposed eDDPC is still applicable in scenarios where limited offline data is available. When sufficiently long PE data is available to allow for application of DDPC and SVD-DDPC schemes (specifically $T \geq (m+1)(L+2n) - 1$), we also use the complete data to test various cases of the eDDPC which arise from the ability to vary the depth d in Algorithm 3. Varying d can be viewed as hyperparameter tuning that can influence the control performance.

Once the data is collected, we can set up the optimization problems for each scheme. Notice that the regularization terms in (24) has the same structure as in the DDPC scheme [9], whereas SVD-DDPC originally included different regularization terms, and the slack variables were only used for the initial conditions (cf. [25]). For consistency, we implement SVD-DDPC using the same structure of the cost function as eDDPC, and use the same number of slack variables as well. For all schemes, the parameters μ_β and μ_σ were set to $\mu_\beta = \mu_\sigma = 0.5$, thus satisfying Assumption 2. The value of the regularization pa-

⁵ The values $T \in \{23, 35, 47, 59, 71\}$ correspond to the minimum number of data points required to build $\mathcal{H}_d(\bar{w})$ for $d \in \{n, 2n, \dots, 5n\}$. For DDPC and SVD-DDPC, only lengths $T \in \{71, 100, 200, 300\}$ were considered as the minimum number of data points is $T \geq (m+1)(L+2n) - 1 = 71$.

Table 2
Optimal values for the regularization parameters λ_β and λ_σ for the SLRA-eDDPC scheme for different values of T .

| d | 4 | 8 | 12 | 16 | 20 | 20 | 20 | 20 |
|--------------------|-----------|-----------|-----|-----|-----|------|------|------|
| T | 23 | 35 | 47 | 59 | 71 | 100 | 200 | 300 |
| λ_β^* | 0 | 0 | 0 | 0.1 | 0.1 | 0.01 | 0.01 | 0.01 |
| λ_σ^* | 10^{-4} | 10^{-2} | 0.1 | 10 | 10 | 10 | 10 | 10 |

rameters $\lambda_\beta, \lambda_\sigma$, however, were varied from one scheme to another and needed to be tuned individually. For the purpose of this example, we empirically determined a pair of “optimal” choice of parameters λ_β and λ_σ for each scheme by varying the regularization parameters over a grid defined by $\lambda_i \in \{0, 10^{-6}, 10^{-5}, \dots, 10^4\}$ for $i = \beta, \sigma$, across all schemes for all different data lengths T . For each scheme and each combination $(\lambda_\beta, \lambda_\sigma, T)$, we performed 100 simulations, using different initial conditions and different offline data sets. An optimal pair $(\lambda_\beta^*, \lambda_\sigma^*)$ for each combination is chosen as the one corresponding to the least average accumulated cost defined as

$$\mathcal{J} = \sum_{t=0}^{T_{\text{sim}}-1} \|u_t - u^s\|_R^2 + \|y_t - y^s\|_Q^2, \quad (30)$$

which sums up the weighted closed-loop input-output trajectories over the simulation time $T_{\text{sim}} = 300$. All simulations were carried out using MATLAB 2023b on an Intel Core i7-10700K CPU with 3.80GHz and 64 GB RAM. The optimization problems were solved using the `quadprog` in Matlab.

For space reasons, we only report the resulting optimal regularization parameters for SLRA-eDDPC in Table 2. It can be observed that λ_σ^* increases with a larger number of data points. A larger regularization parameter corresponds to less relaxation of (24b), potentially due to a more accurate predictor which is obtained after performing the necessary pre-processing steps of Algorithm 1 on a deeper Hankel matrix, i.e., larger d . This suggests that using more offline data yields a more accurate predictor. For λ_β^* , it can be seen that this parameter attains small values regardless of the number of data points T . A possible explanation for not largely regularizing $\hat{\beta}(t)$ is that the pre-processing steps used in Algorithm 1 have a denoising effect on the data matrix (similarly also for SVD-DDPC). In contrast, DDPC directly uses the Hankel matrix of noisy data and, hence, regularization of the regressor vector is needed.

Remark 15 *We include 0 in the hyperparameter space which turned out to be an optimal choice for some depths d (see Table 2). Theorem 14, however, requires that $\lambda_\beta, \lambda_\sigma > 0$. To maintain theoretical guarantees, one may choose λ_β to be a small number rather than zero in those cases, which does not largely affect the closed-loop cost.*

After tuning the hyperparameters, we proceed to investigate the impact of varying the number of data points

T and noise levels $\bar{\varepsilon}$ in a new simulation. To this end, we consider the same choices for the number of data points as before and, for each such T , conducted 100 simulation experiments using newly collected offline noisy data and new initial conditions. The resulting accumulated closed-loop costs, averaged over 100 experiments, are presented in Figure 1. It can be seen that SLRA-eDDPC outperforms the other schemes when small amounts of data are used. This is measured in terms of the accumulated closed-loop cost (30), which attains a minimum of around 43.5. Notice that when $T = 59$ DDPC and SVD-DDPC cannot be implemented, whereas SLRA-eDDPC results in comparable performance to that of DDPC and SVD-DDPC that use $T \geq 100$ data points. When using TSVD, eDDPC achieves good performance with 100 data points. DDPC and SVD-DDPC show similar performance to eDDPC for $T \geq 71$, which is the minimum data length for these schemes. As T increases, all schemes show comparable performance. The results in Figure 1 highlight that (i) the SLRA-eDDPC scheme performs well when small number of noisy data is available offline and (ii) the use of SLRA is better suited than TSVD when dealing with noisy data.

Finally, we investigate the effect of various noise levels on the performance of the different schemes. To this end, we fixed the number of data points at $T = 200$ and conducted 100 simulations for the noise levels $\bar{\varepsilon} \in \{10^{-3}, 4 \cdot 10^{-3}, 7 \cdot 10^{-3}, 10^{-2}\}$. The averaged accumulated costs are shown in Figure 2. The results show that SLRA-eDDPC consistently achieves the lowest cost \mathcal{J} , followed by eDDPC, SVD-DDPC and DDPC. This trend becomes more prominent with increasing noise levels, which further highlights the denoising effect of SLRA.

7 Conclusions

In this paper, we presented a robust and efficient data-driven predictive control scheme for discrete-time linear time-invariant systems. As with other DDPC schemes, no model knowledge is available and, instead, only noisy input-output data are available from an offline experiment. This scheme is more sample efficient (requires less offline data) compared to existing schemes, and is also computationally efficient. This is due to its reliance on an alternative data-based representation of the finite-length behavior of the system which can be obtained from short (and potentially irregularly measured) noisy data. This makes the proposed eDDPC scheme applicable in cases where existing schemes fail due to limited/missing offline data.

For our proposed robust eDDPC, we proved recursive feasibility and practical stability of the closed-loop system, unlike recent literature on efficient DDPC that lack theoretical guarantees. To do so, we introduced a novel result on uncertainty quantification in the behavioral framework. In particular, we derived a bound on the an-

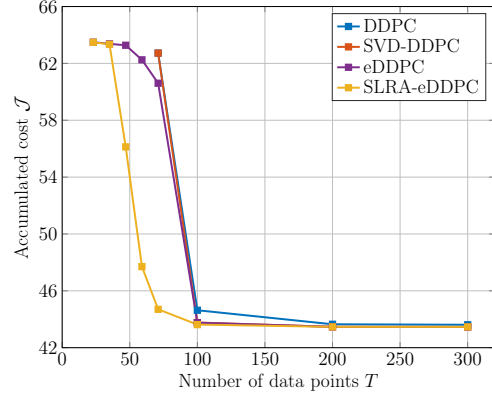


Fig. 1. Accumulated closed-loop costs averaged over 100 simulations, with varying number of data points T and noise level $\bar{\varepsilon} = 0.004$ for all schemes.

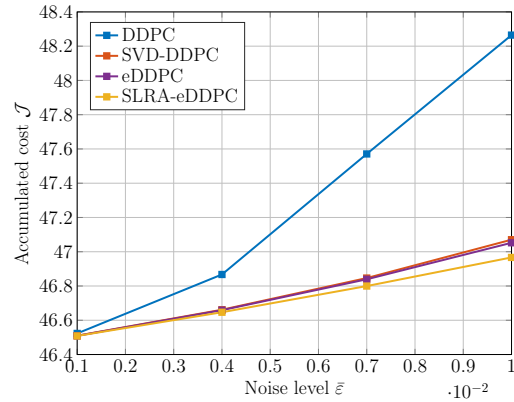


Fig. 2. Accumulated closed-loop costs, averaged over 100 simulations, with varying noise levels $\bar{\varepsilon}$ and $T = 200$ data points for all schemes.

gle between two subspaces: the unknown finite-length behavior of the system and its known approximation from noisy input-output data. Under certain conditions, this bound goes to zero as the noise level tends to zero.

To illustrate the performance of this scheme compared to others in the literature, we conducted a simulation case study on a linearized model of four tank system. Our results show that, when sufficiently long PE data is available, the scheme performs similarly to existing ones from the literature. When significantly less data is available, however, none of the other existing DDPC schemes can be applied. In contrast, our eDDPC scheme is still applicable and results in comparable performance to the case when long enough data is available, in the sense that the accumulated closed-loop costs are very close to one another.

Several extensions of the proposed eDDPC scheme can be made. For instance, we considered regulation of constant set points but the scheme can be extended to tracking DDPC as in [12]. Moreover, output constraint satisfaction (e.g., as in [37]) is not considered in this paper

but is an important topic for future research. Finally, applying the proposed scheme to real-world systems is another interesting venue for future work.

Acknowledgements

This work has received funding from the European Research Council (ERC) under the European Union's Horizon 2020 research and innovation programme (grant agreement No 948679).

References

- [1] J. Rawlings, D. Mayne, and M. Diehl, *Model Predictive Control: Theory, Computation, and Design*. Nob Hill Publishing, 2017.
- [2] L. Hewing, K. P. Wabersich, M. Menner, and M. N. Zeilinger, "Learning-based model predictive control: Toward safe learning in control," *Annual Review of Control, Robotics, and Autonomous Systems*, vol. 3, pp. 269–296, 2020.
- [3] J. C. Willems, "From time series to linear system—parts I–III," *Automatica*, vol. 22, no. 5, 1986.
- [4] J. C. Willems, P. Rapisarda, I. Markovskiy, and B. L. De Moor, "A note on persistency of excitation," *Systems & Control Letters*, vol. 54, no. 4, pp. 325–329, 2005.
- [5] I. Markovskiy and F. Dörfler, "Identifiability in the behavioral setting," *IEEE Transactions on Automatic Control*, vol. 68, no. 3, pp. 1667–1677, 2022.
- [6] J. Coulson, J. Lygeros, and F. Dörfler, "Data-enabled predictive control: In the shallows of the DeePC," in *2019 18th European Control Conference (ECC)*, pp. 307–312, 2019.
- [7] J. Coulson, J. Lygeros, and F. Dörfler, "Distributionally robust chance constrained data-enabled predictive control," *IEEE Transactions on Automatic Control*, vol. 67, no. 7, pp. 3289–3304, 2022.
- [8] J. Berberich, J. Köhler, M. A. Müller, and F. Allgöwer, "Data-driven model predictive control with stability and robustness guarantees," *IEEE Transactions on Automatic Control*, vol. 66, no. 4, pp. 1702–1717, 2021.
- [9] J. Berberich, J. Köhler, M. A. Müller, and F. Allgöwer, "Stability in data-driven MPC: an inherent robustness perspective," in *2022 IEEE 61st Conference on Decision and Control (CDC)*, pp. 1105–1110, 2022.
- [10] C. Verhoek, H. Abbas, R. Tóth, and S. Haesaert, "Data-driven predictive control for linear parameter-varying systems," *IFAC-PapersOnLine*, vol. 54, no. 8, pp. 101–108, 2021.
- [11] Y. Lian and C. N. Jones, "Nonlinear data-enabled prediction and control," in *PMLR*, vol. 144, pp. 523–534, 2021.
- [12] J. Berberich, J. Köhler, M. A. Müller, and F. Allgöwer, "Linear tracking MPC for nonlinear systems-part II: The data-driven case," *IEEE Transactions on Automatic Control*, vol. 67, no. 9, pp. 4406–4421, 2022.
- [13] M. Alsalti, V. G. Lopez, J. Berberich, F. Allgöwer, and M. A. Müller, "Data-driven nonlinear predictive control for feedback linearizable systems," *IFAC-PapersOnLine*, vol. 56, no. 2, pp. 617–624, 2023.
- [14] M. Lazar, "Basis-functions nonlinear data-enabled predictive control: Consistent and computationally efficient formulations," in *2024 European Control Conference (ECC)*, pp. 888–893, 2024.
- [15] G. Pan, R. Ou, and T. Faulwasser, "On a stochastic fundamental lemma and its use for data-driven optimal control," *IEEE Transactions on Automatic Control*, vol. 68, no. 10, pp. 5922–5937, 2023.
- [16] V. Breschi, A. Chiuso, and S. Formentin, "Data-driven predictive control in a stochastic setting: a unified framework," *Automatica*, vol. 152, p. 110961, 2023.
- [17] M. Köhler, J. Berberich, M. A. Müller, and F. Allgöwer, "Data-driven distributed MPC of dynamically coupled linear systems," *IFAC-PapersOnLine*, vol. 55, no. 30, pp. 365–370, 2022.
- [18] C. A. Alonso, F. Yang, and N. Matni, "Data-driven distributed and localized model predictive control," *IEEE Open Journal of Control Systems*, vol. 1, pp. 29–40, 2022.
- [19] F. Dörfler, J. Coulson, and I. Markovskiy, "Bridging direct and indirect data-driven control formulations via regularizations and relaxations," *IEEE Transactions on Automatic Control*, vol. 68, no. 2, pp. 883–897, 2023.
- [20] V. Breschi and S. Formentin, "AutoDDC: Hyperparameter tuning for direct data-driven control," *IEEE Control Systems Magazine*, vol. 43, no. 6, pp. 98–124, 2023.
- [21] I. Markovskiy, L. Huang, and F. Dörfler, "Data-driven control based on the behavioral approach: From theory to applications in power systems," *IEEE Control Systems Magazine*, vol. 43, no. 5, pp. 28–68, 2023.
- [22] E. Elokda, J. Coulson, P. N. Beuchat, J. Lygeros, and F. Dörfler, "Data-enabled predictive control for quadcopters," *International Journal of Robust and Nonlinear Control*, vol. 31, no. 18, pp. 8916–8936, 2021.
- [23] P. Verheijen, V. Breschi, and M. Lazar, "Handbook of linear data-driven predictive control: Theory, implementation and design," *Annual Reviews in Control*, vol. 56, p. 100914, 2023.
- [24] E. O'Dwyer, E. C. Kerrigan, P. Falugi, M. Zagorowska, and N. Shah, "Data-driven predictive control with improved performance using segmented trajectories," *IEEE Transactions on Control Systems Technology*, vol. 31, no. 3, pp. 1355–1365, 2023.
- [25] K. Zhang, Y. Zheng, C. Shang, and Z. Li, "Dimension reduction for efficient data-enabled predictive control," *IEEE Control Systems Letters*, vol. 7, pp. 3277–3282, 2023.
- [26] M. Alsalti, I. Markovskiy, V. G. Lopez, and M. A. Müller, "Data-based system representations from irregularly measured data," *IEEE Trans. Autom. Control*, 2024.
- [27] M. Alsalti, M. Barkey, V. G. Lopez, and M. A. Müller, "Sample-and computationally efficient data-driven predictive control," in *22nd European Control Conference (ECC)*, pp. 84–89, 2024.
- [28] G. Stewart, "Perturbation theory for the singular value decomposition," *SVD and Signal Processing II, Algorithms, Analysis and Applications*, pp. 99–109, 1991.
- [29] A. Padoan, J. Coulson, H. J. van Waarde, J. Lygeros, and F. Dörfler, "Behavioral uncertainty quantification for data-driven control," in *2022 IEEE 61st Conference on Decision and Control (CDC)*, pp. 4726–4731, 2022.
- [30] A. Fazzi and I. Markovskiy, "Distance problems in the behavioral setting," *Eur. J. Control*, p. 100832, 2023.
- [31] C. Eckart and G. Young, "The approximation of one matrix by another of lower rank," *Psychometrika*, vol. 1, no. 3, pp. 211–218, 1936.
- [32] I. Markovskiy, "Structured low-rank approximation and its applications," *Automatica*, vol. 44, no. 4, pp. 891–909, 2008.
- [33] A. J. Sasane, "Distance between behaviours," *International Journal of Control*, vol. 76, no. 12, pp. 1214–1223, 2003.

- [34] J. Miao and A. Ben-Israel, "On principal angles between subspaces in \mathbb{R}^n ," *Linear Algebra and its Applications*, vol. 171, pp. 81–98, 1992.
- [35] J. Coulson, H. J. v. Waarde, J. Lygeros, and F. Dörfler, "A quantitative notion of persistency of excitation and the robust fundamental lemma," *IEEE Control Systems Letters*, vol. 7, pp. 1243–1248, 2023.
- [36] V. Breschi, A. Chiuso, M. Fabris, and S. Formentin, "On the impact of regularization in data-driven predictive control," in *2023 62nd IEEE Conference on Decision and Control (CDC)*, pp. 3061–3066, 2023.
- [37] C. Klöppelt, J. Berberich, F. Allgöwer, and M. A. Müller, "A novel constraint-tightening approach for robust data-driven predictive control," *International Journal of Robust and Nonlinear Control*, 2022.
- [38] G. C. Goodwin and K. S. Sin, *Adaptive filtering prediction and control*. Dover Publications, 2014.
- [39] C. Cai and A. R. Teel, "Input–output-to-state stability for discrete-time systems," *Automatica*, vol. 44, no. 2, pp. 326–336, 2008.
- [40] A. Bemporad, M. Morari, V. Dua, and E. N. Pistikopoulos, "The explicit linear quadratic regulator for constrained systems," *Automatica*, vol. 38, no. 1, pp. 3–20, 2002.
- [41] L. Grüne and M. Stieler, "Asymptotic stability and transient optimality of economic MPC without terminal conditions," *J. Process Control*, vol. 24, no. 8, pp. 1187–1196, 2014.

A Proof of Lemma 8

Recall from the discussion below Definition 3 that principal vectors defining the bases of two subspaces (here $\text{im}(U_M)$ and $\text{im}(U_{\widehat{M}})$) always exist. Let the columns of \overline{U}_M and $\overline{U}_{\widehat{M}}$ be such principal vectors satisfying $\text{im}(\overline{U}_M) = \text{im}(U_M)$ and $\text{im}(\overline{U}_{\widehat{M}}) = \text{im}(U_{\widehat{M}})$, respectively. Consequently, there exists a matrix $G = [g_1 \cdots g_r] \in \mathbb{R}^{r \times r}$ such that $U_{\widehat{M}} = \overline{U}_{\widehat{M}}G$. Recall that the columns of $U_{\widehat{M}} = [u_{\widehat{M},1} \cdots u_{\widehat{M},r}]$ are orthonormal and, as a result, the following holds

$$\begin{aligned} u_{\widehat{M},i}^\top u_{\widehat{M},j} &= 0 \implies g_i^\top \overline{U}_M^\top \overline{U}_{\widehat{M}} g_j = g_i^\top g_j = 0, \quad \forall i \neq j, \\ u_{\widehat{M},i}^\top u_{\widehat{M},i} &= 1 \implies g_i^\top \overline{U}_M^\top \overline{U}_{\widehat{M}} g_i = g_i^\top g_i = 1, \end{aligned} \quad (\text{A.1})$$

where $\overline{U}_M^\top \overline{U}_{\widehat{M}} = I_r$ holds by definition of the principal vectors. Notice that (A.1) also implies that the matrix G is orthogonal. Letting $\widetilde{U}_M := \overline{U}_M G$ we obtain a basis for $\text{im}(U_M)$ as desired. Since \widetilde{U}_M is the product of two orthogonal matrices, it is orthogonal as well.

Now, it remains to be shown that (17) holds. Using (the given) $U_{\widehat{M}}$ and (the constructed) \widetilde{U}_M , we write

$$\begin{aligned} \|\widetilde{U}_M - U_{\widehat{M}}\|_F &= \|\overline{U}_M G - \overline{U}_{\widehat{M}} G\|_F = \|(\overline{U}_M - \overline{U}_{\widehat{M}})G\|_F \\ &\leq \|\overline{U}_M - \overline{U}_{\widehat{M}}\|_F \|G\|_F \leq \sqrt{r} \|\overline{U}_M - \overline{U}_{\widehat{M}}\|_F, \end{aligned} \quad (\text{A.2})$$

where the last inequality follows from $\|G\|_F = \sqrt{\sum_{i=1}^r \|g_i\|_2^2} = \sqrt{r}$ since $g_i^\top g_i = 1$ as in (A.1). Now consider a pair of vectors $\bar{u}_{M,j}, \bar{u}_{\widehat{M},j}$ which are columns of $\overline{U}_M, \overline{U}_{\widehat{M}}$, respectively. By definition of the 2-norm, we have $\|\bar{u}_{M,j} - \bar{u}_{\widehat{M},j}\|_2^2 = (\bar{u}_{M,j} - \bar{u}_{\widehat{M},j})^\top (\bar{u}_{M,j} - \bar{u}_{\widehat{M},j})$, or

$$\|\bar{u}_{M,j} - \bar{u}_{\widehat{M},j}\|_2^2 = 2(1 - \bar{u}_{M,j}^\top \bar{u}_{\widehat{M},j}) = 2(1 - \cos \theta_j),$$

where $\bar{u}_{M,j}^\top \bar{u}_{M,j} = \bar{u}_{\widehat{M},j}^\top \bar{u}_{\widehat{M},j} = 1$ and $\cos \theta_j = \bar{u}_{M,j}^\top \bar{u}_{\widehat{M},j}$ hold since the vectors $\bar{u}_{M,j}, \bar{u}_{\widehat{M},j}$ are principal vectors (cf. (14)). Using the identity $\sin^2\left(\frac{\theta_j}{2}\right) = \frac{1 - \cos \theta_j}{2}$ we get

$$\|\bar{u}_{M,j} - \bar{u}_{\widehat{M},j}\|_2^2 = 4 \sin^2(\theta_j/2) \leq 4 \sin^2 \theta_j, \quad (\text{A.3})$$

where the last inequality holds for all $\theta_j \in [0, \frac{2\pi}{3}]$, and hence also for $\theta_j \in [0, \frac{\pi}{2}]$ (which are the limits of θ_j as defined in Definition 3). Summing over $j \in \{1, \dots, r\}$ on both sides and taking the square root, we obtain

$$\sqrt{\sum_{j=1}^r \|\bar{u}_{M,j} - \bar{u}_{\widehat{M},j}\|_2^2} \leq \sqrt{\sum_{j=1}^r 4 \sin^2 \theta_j} = 2 \sqrt{\sum_{j=1}^r \sin^2 \theta_j}.$$

Notice that the leftmost side corresponds to the Frobenius norm of the difference between the bases \overline{U}_M and $\overline{U}_{\widehat{M}}$, while the right hand side corresponds to the Frobenius norm of the diagonal matrix $\sin \Theta(\text{im}(U_M), \text{im}(U_{\widehat{M}}))$. Hence, $\|\overline{U}_M - \overline{U}_{\widehat{M}}\|_F \leq 2 \|\sin \Theta(\text{im}(U_M), \text{im}(U_{\widehat{M}}))\|_F$. Plugging this back into (A.2) results in

$$\|\widetilde{U}_M - U_{\widehat{M}}\|_F \leq 2\sqrt{r} \|\sin \Theta(\text{im}(U_M), \text{im}(U_{\widehat{M}}))\|_F,$$

which completes the proof. \blacksquare

B Proof of Theorem 9

Since $\text{rank}(\mathcal{H}_d(\tilde{w})) \geq \text{rank}(\mathcal{H}_d(w)) = md + n$, then one can perform a TSVD approximation as in (11) to obtain $\widehat{\mathcal{H}}$ with $\text{rank}(\widehat{\mathcal{H}}) = md + n$. Moreover, a basis for the left null space of the two matrices are given by $R_d = \text{null}(\mathcal{H}_d(w)^\top)^\top$ and $\widehat{R}_d = \text{null}(\widehat{\mathcal{H}}^\top)^\top$, respectively. Using $(L + n - d)$ shifts of R_d and \widehat{R}_d , one can build Γ and $\widehat{\Gamma}$ as in (6), the SVD of which is denoted by

$$\begin{aligned} \Gamma &= [U_\Gamma \ W_\Gamma] \text{diag}(S_\Gamma, 0) [V_\Gamma \ Q_\Gamma]^\top, \\ \widehat{\Gamma} &= [U_{\widehat{\Gamma}} \ W_{\widehat{\Gamma}}] \text{diag}(S_{\widehat{\Gamma}}, 0) [V_{\widehat{\Gamma}} \ Q_{\widehat{\Gamma}}]^\top, \end{aligned} \quad (\text{B.1})$$

where $S_\Gamma = \text{diag}(s_1(\Gamma), \dots, s_{p(L+n)-n}(\Gamma))$ and $S_{\widehat{\Gamma}} = \text{diag}(s_1(\widehat{\Gamma}), \dots, s_{p(L+n)-n}(\widehat{\Gamma}))$ (both of which have rank

$p(L+n)-n$ by construction, see also [26] for details). Further, U_i, W_i, V_i, Q_i (for $i = \{\Gamma, \widehat{\Gamma}\}$) are semi-orthonormal matrices of appropriate dimensions. By Theorem 7,⁶

$$\|\sin(\Theta(\text{im}(Q_\Gamma), \text{im}(Q_{\widehat{\Gamma}})))\|_F \leq \frac{\sqrt{2}}{\delta_1} \|E\|_F, \quad (\text{B.2})$$

where $\delta_1 = s_{p(L+n)-n}(\widehat{\Gamma})$ and $E := \widehat{\Gamma} - \Gamma$. By properties of the SVD, it holds that $\text{im}(Q_\Gamma) = \ker(\Gamma) = \text{im}(P) = \mathcal{B}|_{L+n}$ where the last equality holds by Theorem 3 (see [26, Th. 3] for more details). Similarly, it holds that $\text{im}(Q_{\widehat{\Gamma}}) = \ker(\widehat{\Gamma}) = \text{im}(\widehat{P}) = \widehat{\mathcal{B}}|_{L+n}$, where the last equality holds by definition of $\widehat{\mathcal{B}}|_{L+n}$ as in the theorem statement. Therefore, we can write (B.2) as

$$\left\| \sin \Theta(\widehat{\mathcal{B}}|_{L+n}, \mathcal{B}|_{L+n}) \right\|_F \leq \frac{\sqrt{2} \|E\|_F}{\delta_1}. \quad (\text{B.3})$$

Moreover, $\|E\|_F = \|\widehat{\Gamma} - \Gamma\|_F = \sqrt{\sum_{i,j} \|e_{i,j}\|^2}$ is given by

$$\|E\|_F = \sqrt{\sum_{i=1}^{pd-n} \sum_{j=0}^{d-1} \|\widehat{r}_{i,j} - r_{i,j}\|^2 + (L+n-d) \sum_{i=1}^p \sum_{j=0}^{d-1} \|\widehat{r}_{i,j} - r_{i,j}\|^2}. \quad (\text{B.4})$$

Since $\sum_{i=1}^p \sum_{j=0}^{d-1} \|\widehat{r}_{i,j} - r_{i,j}\|^2 \leq \sum_{i=1}^{pd-n} \sum_{j=0}^{d-1} \|\widehat{r}_{i,j} - r_{i,j}\|^2$, we can write

$$\begin{aligned} \|E\|_F &\leq \sqrt{(L+n-d+1) \sum_{i=1}^{pd-n} \sum_{j=0}^{d-1} \|\widehat{r}_{i,j} - r_{i,j}\|^2} \\ &= \underbrace{\sqrt{L+n-d+1}}_{:=c_1} \|\widehat{R}_d - R_d\|_F. \end{aligned} \quad (\text{B.5})$$

Plugging back in (B.3), we obtain

$$\|\sin \Theta(\widehat{\mathcal{B}}|_{L+n}, \mathcal{B}|_{L+n})\|_F \leq \frac{\sqrt{2}c_1 \|\widehat{R}_d - R_d\|_F}{\delta_1}. \quad (\text{B.6})$$

Now consider the SVD of $\mathcal{H}_d(w)$ and $\widehat{\mathcal{H}}$

$$\begin{aligned} \mathcal{H}_d(w) &= \begin{bmatrix} U_H & W_H \end{bmatrix} \text{diag}(S_H, 0) \begin{bmatrix} V_H & Q_H \end{bmatrix}^\top, \\ \widehat{\mathcal{H}} &= \begin{bmatrix} U_{\widehat{H}} & W_{\widehat{H}} \end{bmatrix} \text{diag}(S_{\widehat{H}}, 0) \begin{bmatrix} V_{\widehat{H}} & Q_{\widehat{H}} \end{bmatrix}^\top, \end{aligned} \quad (\text{B.7})$$

where $S_H = \text{diag}(s_1(\mathcal{H}_d(w)), \dots, s_{md+n}(\mathcal{H}_d(w)))$, $S_{\widehat{H}} = \text{diag}(s_1(\widehat{\mathcal{H}}), \dots, s_{md+n}(\widehat{\mathcal{H}}))$, U_i, W_i, V_i, Q_i (for

⁶ As mentioned before Theorem 7, the bound in (15) holds for all four singular subspaces, see [28].

$i = \{H, \widehat{H}\}$) are semi-orthonormal matrices of appropriate dimensions and W_H is such that (cf. Lemma 8)

$$\|W_{\widehat{H}} - W_H\|_F \leq 2\sqrt{md+n} \|\sin \Theta(\text{im}(W_{\widehat{H}}), \text{im}(W_H))\|_F. \quad (\text{B.8})$$

By Theorem 7, the following holds

$$\left\| \sin \Theta(\text{im}(W_{\widehat{H}}), \text{im}(W_H)) \right\|_F \leq \frac{\sqrt{2} \|\widehat{\mathcal{H}} - \mathcal{H}_d(w)\|_F}{\delta_2}, \quad (\text{B.9})$$

where $\delta_2 = s_{md+n}(\widehat{\mathcal{H}}) = s_{md+n}(\mathcal{H}_d(\tilde{w}))$, which is also non-zero since $\text{rank}(\mathcal{H}_d(\tilde{w})) \geq \text{rank}(\mathcal{H}_d(w)) = md+n > 0$. Notice that the norm on the right hand side of (B.9) can be further bounded by

$$\begin{aligned} \|\widehat{\mathcal{H}} - \mathcal{H}_d(w)\|_F &= \|\widehat{\mathcal{H}} - \mathcal{H}_d(\tilde{w}) + \mathcal{H}_d(\tilde{w}) - \mathcal{H}_d(w)\|_F \\ &\leq \|\widehat{\mathcal{H}} - \mathcal{H}_d(\tilde{w})\|_F + \|\mathcal{H}_d(\tilde{w}) - \mathcal{H}_d(w)\|_F \\ &= \|\widehat{\mathcal{H}} - \mathcal{H}_d(\tilde{w})\|_F + \|\mathcal{H}_d(\epsilon)\|_F. \end{aligned} \quad (\text{B.10})$$

The first term on the right hand side corresponds to the difference between a matrix and its TSVD approximation, which is known to be bounded by the sum of the truncated singular values [28], hence

$$\begin{aligned} \|\widehat{\mathcal{H}} - \mathcal{H}_d(w)\|_F &\leq \sqrt{\sum_{i=md+n+1}^{\text{rank}(\mathcal{H}_d(\tilde{w}))} (s_i(\mathcal{H}_d(\tilde{w})))^2} \\ &\quad + \|\mathcal{H}_d(\epsilon)\|_F. \end{aligned} \quad (\text{B.11})$$

Note that by Theorem 6, the following holds $\|\mathcal{H}_d(\epsilon)\|_F^2 \geq \sum_{i=1}^{\text{rank}(\mathcal{H}_d(\tilde{w}))} (s_i(\mathcal{H}_d(\tilde{w})) - s_i(\mathcal{H}_d(w)))^2$, or

$$\begin{aligned} \|\mathcal{H}_d(\epsilon)\|_F^2 &\leq \sum_{i=1}^{md+n} (s_i(\mathcal{H}_d(\tilde{w})) - s_i(\mathcal{H}_d(w)))^2 \\ &\quad + \sum_{i=md+n+1}^{\text{rank}(\mathcal{H}_d(\tilde{w}))} (s_i(\mathcal{H}_d(\tilde{w})))^2, \end{aligned}$$

where in the last step we exploited the fact that $\text{rank}(\mathcal{H}_d(w)) = md+n$ and hence $s_i(\mathcal{H}_d(w)) = 0$ for $i \geq md+n+1$. It is easy to see from here that

$$\sum_{i=md+n+1}^{\text{rank}(\mathcal{H}_d(\tilde{w}))} (s_i(\mathcal{H}_d(\tilde{w})))^2 \leq \|\mathcal{H}_d(\epsilon)\|_F^2, \quad (\text{B.12})$$

Taking the square root and substituting in (B.11) yields

$$\|\widehat{\mathcal{H}} - \mathcal{H}_d(w)\|_F \leq 2\|\mathcal{H}_d(\epsilon)\|_F \leq 2\sqrt{qd(T-d+1)}\bar{\epsilon}, \quad (\text{B.13})$$

for $q = m+p$, where the last inequality holds by definition of the Frobenius norm along with the fact that $\|\epsilon_k\|_\infty = \|\epsilon_k\|_\infty \leq \bar{\epsilon}$ for all $k \geq 0$ (cf. (9)). Finally, we substitute back in (B.9) to obtain

$$\left\| \sin \Theta(\text{im}(W_{\widehat{H}}), \text{im}(W_H)) \right\|_F \leq \frac{2\sqrt{2qd(T-d+1)}\bar{\epsilon}}{\delta_2}. \quad (\text{B.14})$$

Recall that \widehat{R}_d and R_d form a basis for the left null spaces of $\mathcal{H}_d(\widehat{w})$ and $\mathcal{H}_d(w)$ respectively, and thus $\widehat{R}_d = W_{\widehat{H}}^\top$ and $R_d = W_H^\top$. This, together with (B.8) and the fact that $\|W_{\widehat{H}} - W_H\|_F = \|W_{\widehat{H}}^\top - W_H^\top\|_F$, allow us to write

$$\begin{aligned} \left\| \widehat{R}_d - R_d \right\|_F &\leq 2\sqrt{md+n} \left\| \sin \Theta(\text{im}(W_{\widehat{H}}), \text{im}(W_H)) \right\|_F \\ &\stackrel{\text{(B.14)}}{\leq} \frac{4\sqrt{2qd(md+n)(T-d+1)}}{\delta_2} \bar{\varepsilon}. \end{aligned} \quad (\text{B.15})$$

Substituting back in (B.6) completes the proof. \blacksquare

C Proof of Theorem 14

C.1 Translating online measurement noise to an input disturbances to the nominal scheme

We start by showing that the online measurement noise in the robust scheme (24) can be viewed as an input disturbance to the nominal scheme (7). The steps followed here are adaptations from the proof of [9, Th. IV.1].

Assume that $V(\xi_t) \leq \bar{V}$ (this will be established recursively later in Section C.3). By definition of $V(\xi_t)$ (see (26)), it follows that $J_L^*(\xi_t) \leq V(\xi_t) \leq \bar{V}$. Now, we proceed by defining a feasible candidate solution for (24) based on the optimal solution of (7). Specifically, let

$$\begin{aligned} \widehat{w}(t) &:= \begin{bmatrix} \widetilde{w}_{[t-n, t-1]}^{\text{on}} \\ \widetilde{w}_{[0, L-1]}^*(t) \end{bmatrix} \stackrel{\text{(9)}}{=} \begin{bmatrix} w_{[t-n, t-1]}^{\text{on}} + \epsilon_{[t-n, t-1]} \\ \widetilde{w}_{[0, L-1]}^*(t) \end{bmatrix} \\ &\stackrel{\text{(7c)}}{=} \widetilde{w}_{[-n, L-1]}^*(t) + \begin{bmatrix} \epsilon_{[t-n, t-1]} \\ 0_{qL \times 1} \end{bmatrix}. \end{aligned} \quad (\text{C.1})$$

Moreover, let $\widehat{\beta}(t) = \beta^*(t)$ where $\beta^*(t)$ satisfies $P\beta^*(t) = \widetilde{w}^*(t)$ (cf. (7b)) for some P satisfying (23). Based on the definitions of $\widehat{w}(t), \widehat{\beta}(t)$, we define the following candidate solution for $\widehat{\sigma}(t)$ as the one which makes (24b) holds, i.e., $\widehat{\sigma}(t) = \widehat{P}\widehat{\beta}(t) - \widehat{w}(t)$. In particular

$$\begin{aligned} \widehat{\sigma}(t) &\stackrel{\text{(C.1)}}{=} \widehat{P}\widehat{\beta}(t) - \widetilde{w}_{[-n, L-1]}^*(t) - \begin{bmatrix} \epsilon_{[t-n, t-1]} \\ 0_{qL \times 1} \end{bmatrix} \\ &\stackrel{\text{(7b)}}{=} \widehat{P}\widehat{\beta}(t) - P\beta^*(t) - \begin{bmatrix} \epsilon_{[t-n, t-1]} \\ 0_{qL \times 1} \end{bmatrix}, \end{aligned} \quad (\text{C.2})$$

or $\widehat{\sigma}(t) = (\widehat{P} - P)\widehat{\beta}(t) - \begin{bmatrix} \epsilon_{[t-n, t-1]} \\ 0_{qL \times 1} \end{bmatrix}$. Taking the norm on both sides allows us to write

$$\begin{aligned} \|\widehat{\sigma}(t)\|_2^2 &\leq \|\widehat{P} - P\|_2^2 \|\widehat{\beta}(t)\|_2^2 + \|\epsilon_{[t-n, t-1]}\|_2^2 \\ &\leq \|\widehat{P} - P\|_F^2 \|\widehat{\beta}(t)\|_2^2 + np\bar{\varepsilon}^2, \end{aligned} \quad (\text{C.3})$$

where the second inequality holds by standard norm

equivalences. Recall from Corollary 12 that

$$\|\widehat{P} - P\|_F \leq \frac{2\sqrt{m(L+n) + nC_\theta/s_{p(L+n)-n}(\Gamma)}}{s_{md+n}(\mathcal{H}_d(w)) - (\bar{\rho}_1 + \bar{\rho}_2)\bar{\varepsilon}} \bar{\varepsilon}. \quad (\text{C.4})$$

For a fixed ε_1 satisfying $0 \leq \varepsilon_1 < \frac{s_{md+n}(\mathcal{H}_d(w))}{(\bar{\rho}_1 + \bar{\rho}_2)}$, there exists some (sufficiently large) constant $c_2 > 0$ such that for all $\varepsilon^* \in [0, \varepsilon_1]$ and all $\bar{\varepsilon} \in [0, \varepsilon^*]$, the following holds $\|\widehat{P} - P\|_F \leq c_2\bar{\varepsilon}$ (which in turn also implies $\|\widehat{P} - P\|_F^2 \leq c_2^2\bar{\varepsilon}^2$). Plugging this back into (C.3), we obtain

$$\|\widehat{\sigma}(t)\|_2^2 \leq c_2^2\bar{\varepsilon}^2 \|\widehat{\beta}(t)\|_2^2 + c_3\bar{\varepsilon}^2, \quad (\text{C.5})$$

where we have defined $c_3 = np$ for convenience.

Now, let $\widehat{J}_L(\widetilde{\xi}_t)$ denote the cost of (24) associated with the candidate solutions $\widehat{w}(t), \widehat{\beta}(t)$ above. By optimality, it holds that $\widehat{J}_L^*(\widetilde{\xi}_t) \leq \widehat{J}_L(\widetilde{\xi}_t)$ where $\widehat{J}_L^*(\widetilde{\xi}_t)$ denotes the optimal cost of (24). Notice that the only difference between $\widehat{J}_L(\widetilde{\xi}_t)$ and the corresponding optimal cost of (7) (i.e., $J_L^*(\xi_t)$) is the regularization terms of the robust eD-DPC Problem (24) (see (7a), (24a) and (C.1)). Together with $\widehat{J}_L^*(\widetilde{\xi}_t) \leq \widehat{J}_L(\widetilde{\xi}_t)$, we write

$$\begin{aligned} \widehat{J}_L^*(\widetilde{\xi}_t) - J_L^*(\xi_t) &\leq \lambda_\beta \bar{\varepsilon}^{\mu_\beta} \|\widehat{\beta}(t)\|_2^2 + \frac{\lambda_\sigma}{\bar{\varepsilon}^{\mu_\sigma}} \|\widehat{\sigma}(t)\|_2^2 \\ &\stackrel{\text{(C.5)}}{\leq} (\lambda_\beta \bar{\varepsilon}^{\mu_\beta} + \lambda_\sigma c_2^2 \bar{\varepsilon}^{2-\mu_\sigma}) \|\widehat{\beta}(t)\|_2^2 + \lambda_\sigma c_3 \bar{\varepsilon}^{2-\mu_\sigma}. \end{aligned}$$

Recall again that $\widehat{\beta}(t) = \beta^*(t)$. This, together with (7b) allows us to write $\widehat{\beta}(t) = P^\dagger \widetilde{w}^*(t)$, where P^\dagger is a left inverse of P (which exists since P has full column rank, cf. Theorem 3). Plugging this expression in the above bound, we obtain $\widehat{J}_L^*(\widetilde{\xi}_t) \leq J_L^*(\xi_t) + (\lambda_\beta \bar{\varepsilon}^{\mu_\beta} + \lambda_\sigma c_2^2 \bar{\varepsilon}^{2-\mu_\sigma}) \|P^\dagger\|_2^2 \|\widetilde{w}^*(t)\|_2^2 + \lambda_\sigma c_3 \bar{\varepsilon}^{2-\mu_\sigma}$. Since only stabilization of the origin is considered, then by (7a) it holds that $\|\widetilde{w}^*(t)\|_2^2 \leq \frac{\|\widetilde{w}^*(t)\|_W^2}{\lambda_{\min}(W)} = \frac{J_L^*(\xi_t)}{\lambda_{\min}(W)} \leq \frac{\bar{V}}{\lambda_{\min}(W)}$. This can now be plugged back in the last inequality to obtain

$$\begin{aligned} \widehat{J}_L^*(\widetilde{\xi}_t) &\leq J_L^*(\xi_t) + (\lambda_\beta \bar{\varepsilon}^{\mu_\beta} + \lambda_\sigma c_2^2 \bar{\varepsilon}^{2-\mu_\sigma}) \|P^\dagger\|_2^2 \frac{\bar{V}}{\lambda_{\min}(W)} \\ &\quad + \lambda_\sigma c_3 \bar{\varepsilon}^{2-\mu_\sigma} =: J_L^*(\xi_t) + \phi_1(\bar{\varepsilon}), \end{aligned} \quad (\text{C.6})$$

where $\phi_1 \in \mathcal{K}_\infty$ due to Assumption 2. This bound will be used in the following subsections to establish an upper bound on $\|\widehat{u}^*(t) - \bar{u}^*(t)\|$.

C.1.1 Bound on $\|\hat{u}^*(t) - \check{u}^*(t)\|$

Consider the following auxiliary optimization problem

$$\min_{\check{\beta}(t), \check{w}(t)} \sum_{k=0}^{L-1} \|\check{w}_k(t)\|_W^2 + \lambda_\beta \bar{\varepsilon}^{\mu_\beta} \|\check{\beta}(t)\|_2^2 \quad (\text{C.7a})$$

$$\text{s.t. } \check{w}_{[-n, L-1]}(t) + \check{\sigma}_1 = P\check{\beta}(t) \quad (\text{C.7b})$$

$$\check{w}_{[-n, -1]}(t) = w_{[t-n, t-1]}^{\text{on}} + \check{\sigma}_2 \quad (\text{C.7c})$$

$$\check{w}_{[L-n, L-1]}(t) = 0_{q_m \times 1} \quad (\text{C.7d})$$

$$\check{w}_k(t) \in \mathbb{W}, \quad \forall k \in \mathbb{Z}_{[0, L-1]}, \quad (\text{C.7e})$$

with the parameter $\check{\sigma}$ defined as

$$\check{\sigma} = \begin{bmatrix} \check{\sigma}_1 \\ \check{\sigma}_2 \end{bmatrix} := \begin{bmatrix} \hat{\sigma}^*(t) - (\hat{P} - P)\hat{\beta}^*(t) \\ \epsilon_{[t-n, t-1]} \end{bmatrix} \quad (\text{C.8})$$

It can be easily verified that a candidate solution to (C.7) is given by the optimal solution of (24) (which exists since (24) is feasible as shown above in Section C.1), i.e., $\check{w}(t) = \hat{w}^*(t)$ and $\check{\beta}(t) = \hat{\beta}^*(t)$. Denote the corresponding cost associated with this candidate solution to (C.7) by $\check{J}_L(\xi_t)$ and let the optimal solutions and the corresponding optimal cost be denoted by $\check{w}^*(t)$, $\check{\beta}^*(t)$ and $\check{J}_L^*(\xi_t)$, respectively. By optimality, it holds that

$$\begin{aligned} \check{J}_L^*(\xi_t) &\leq \check{J}_L(\xi_t) \stackrel{(\text{C.7a})}{=} \sum_{k=0}^{L-1} \|\check{w}_k(t)\|_W^2 + \lambda_\beta \bar{\varepsilon}^{\mu_\beta} \|\check{\beta}(t)\|_2^2 \\ &= \sum_{k=0}^{L-1} \|\hat{w}_k^*(t)\|_W^2 + \lambda_\beta \bar{\varepsilon}^{\mu_\beta} \|\hat{\beta}^*(t)\|_2^2 \\ &\stackrel{(24a)}{=} \hat{J}_L^*(\tilde{\xi}_t) - \frac{\lambda_\sigma}{\bar{\varepsilon}^{\mu_\sigma}} \|\hat{\sigma}^*(t)\|_2^2. \end{aligned} \quad (\text{C.9})$$

Similarly, one can define a candidate solution for (24) in terms of the optimal solution of (C.7) (which exists according to (C.9)). In particular, define candidate solutions for (24) as $\hat{w}(t) = \check{w}^*(t)$, $\hat{\beta}(t) = \check{\beta}^*(t)$ and

$$\begin{aligned} \hat{\sigma}(t) &= (\hat{P} - P)\hat{\beta}(t) + \check{\sigma}_1 \\ &\stackrel{(\text{C.8})}{=} \hat{\sigma}^*(t) + (\hat{P} - P)(\hat{\beta}(t) - \hat{\beta}^*(t)). \end{aligned} \quad (\text{C.10})$$

Denote the corresponding cost associated with this candidate solution to (24) as $\hat{J}_L^*(\tilde{\xi}_t)$. Notice now that the cost $\hat{J}_L^*(\tilde{\xi}_t)$ differs from the optimal cost of (C.7) by the regularization term involving the slack variable, i.e.,

$$\hat{J}_L^*(\tilde{\xi}_t) - \check{J}_L^*(\xi_t) = \frac{\lambda_\sigma}{\bar{\varepsilon}^{\mu_\sigma}} \|\hat{\sigma}(t)\|_2^2. \quad (\text{C.11})$$

Furthermore, since (24) is strongly convex in \hat{u} , there exists $c_4 > 0$ such that $\|\hat{u}^*(t) - \hat{u}(t)\|_2^2 \leq c_4(\hat{J}_L^*(\tilde{\xi}_t) - \check{J}_L^*(\xi_t)) \stackrel{(\text{C.9})}{\leq} c_4(\hat{J}_L^*(\tilde{\xi}_t) - \check{J}_L^*(\xi_t) - \frac{\lambda_\sigma}{\bar{\varepsilon}^{\mu_\sigma}} \|\hat{\sigma}^*(t)\|_2^2)$. Using

the fact that $\hat{u}(t) = \check{u}^*(t)$ (see definition before (C.10)), together with (C.11) this implies that

$$\|\hat{u}^*(t) - \check{u}^*(t)\|_2^2 \leq c_4 \frac{\lambda_\sigma}{\bar{\varepsilon}^{\mu_\sigma}} (\|\hat{\sigma}(t)\|_2^2 - \|\hat{\sigma}^*(t)\|_2^2).$$

Using (C.10) and $\|a\|_2^2 - \|b\|_2^2 \leq \|a - b\|_2^2 + 2\|a - b\|_2 \|b\|_2$ for $a, b \in \mathbb{R}$, we have $\|\hat{u}^*(t) - \check{u}^*(t)\|_2^2 \leq c_4 \frac{\lambda_\sigma}{\bar{\varepsilon}^{\mu_\sigma}} (\|\hat{\sigma}(t)\|_2^2 - \|\hat{\sigma}^*(t)\|_2^2)$, or

$$\begin{aligned} \|\hat{u}^*(t) - \check{u}^*(t)\|_2^2 &\leq c_4 \frac{\lambda_\sigma}{\bar{\varepsilon}^{\mu_\sigma}} \left(\|\hat{P} - P\|_2^2 \|\hat{\beta}(t) - \hat{\beta}^*(t)\|_2^2 \right. \\ &\quad \left. + 2\|\hat{P} - P\|_2 \|\hat{\beta}(t) - \hat{\beta}^*(t)\|_2 \|\hat{\sigma}^*(t)\|_2 \right). \end{aligned}$$

Now, we use the result of Corollary 12 to bound the term $\|\hat{P} - P\|_2 \leq \|\hat{P} - P\|_F$ which, as in the discussion below (C.4), can be bounded by $c_2 \bar{\varepsilon}$ for any $\bar{\varepsilon} \leq \varepsilon^*$ and any $\varepsilon^* \leq \varepsilon_1$. Moreover, notice that $\|\hat{\beta}^*(t)\|_2^2 \leq \frac{\hat{J}_L^*(\tilde{\xi}_t)}{\lambda_\beta \bar{\varepsilon}^{\mu_\beta}}$ by the optimal cost of (24), whereas $\hat{\beta}(t) = \check{\beta}^*(t)$ (see before (C.10)) which implies that $\|\hat{\beta}(t)\|_2^2 = \|\check{\beta}^*(t)\|_2^2 \leq \frac{\check{J}_L^*(\xi_t)}{\lambda_\beta \bar{\varepsilon}^{\mu_\beta}} \stackrel{(\text{C.9})}{\leq} \frac{\hat{J}_L^*(\tilde{\xi}_t)}{\lambda_\beta \bar{\varepsilon}^{\mu_\beta}}$. Similarly, it holds that $\|\hat{\sigma}^*(t)\|_2^2 \leq \frac{\bar{\varepsilon}^{\mu_\sigma} \hat{J}_L^*(\tilde{\xi}_t)}{\lambda_\sigma}$. Collecting all this together results in

$$\begin{aligned} &\|\hat{u}^*(t) - \check{u}^*(t)\|_2^2 \quad (\text{C.12}) \\ &\leq \frac{2\lambda_\sigma c_4 c_2^2 \bar{\varepsilon}^2}{\lambda_\beta \bar{\varepsilon}^{\mu_\sigma + \mu_\beta}} \hat{J}_L^*(\tilde{\xi}_t) + \frac{4\lambda_\sigma c_4 c_2 \bar{\varepsilon}}{\bar{\varepsilon}^{\mu_\sigma} \sqrt{\lambda_\beta \lambda_\sigma \bar{\varepsilon}^{\mu_\sigma + \mu_\beta}}} \hat{J}_L^*(\tilde{\xi}_t) \\ &=: \left(c_5 \bar{\varepsilon}^{2-\mu_\beta-\mu_\sigma} + c_6 \bar{\varepsilon}^{0.5(2-\mu_\sigma-\mu_\beta)} \right) \hat{J}_L^*(\tilde{\xi}_t) \\ &\stackrel{(\text{C.6})}{\leq} \left(c_5 \bar{\varepsilon}^{2-\mu_\beta-\mu_\sigma} + c_6 \bar{\varepsilon}^{0.5(2-\mu_\sigma-\mu_\beta)} \right) (J_L^*(\xi_t) + \phi_1(\bar{\varepsilon})) \\ &\leq \left(c_5 \bar{\varepsilon}^{2-\mu_\beta-\mu_\sigma} + c_6 \bar{\varepsilon}^{0.5(2-\mu_\sigma-\mu_\beta)} \right) (\bar{V} + \phi_1(\bar{\varepsilon})). \end{aligned}$$

Finally, taking the square root on both sides results in

$$\begin{aligned} \|\hat{u}^*(t) - \check{u}^*(t)\|_2 &\leq \phi_2(\bar{\varepsilon}) \quad (\text{C.13}) \\ &=: \sqrt{\left(c_5 \bar{\varepsilon}^{2-\mu_\beta-\mu_\sigma} + c_6 \bar{\varepsilon}^{0.5(2-\mu_\sigma-\mu_\beta)} \right) (\bar{V} + \phi_1(\bar{\varepsilon}))} \end{aligned}$$

where $\phi_2 \in \mathcal{K}_\infty$ due to Assumption 2.

C.1.2 Bound on $\|\check{u}^*(t) - u'^*(t)\|$

Consider a modification of the minimization problem (C.7) where $\check{\sigma} \equiv 0$. Such a problem has the same structure as (7) but with one additional term in the cost function, namely $\lambda_\beta \bar{\varepsilon}^{\mu_\beta} \|\check{\beta}(t)\|_2^2$. Let the optimal solution of such a problem at time t be denoted by $u'^*(t)$, which exists as implied by the feasibility of (7) at time t (see above). To obtain a bound on $\|\check{u}^*(t) - u'^*(t)\|$, we can follow the same arguments in [9]. In particular, there ex-

ists $c_7 > 0$ such that

$$\begin{aligned} & \|\check{u}^*(t) - u'^*(t)\|_2 \leq c_7 \|\check{\sigma}\|_2 \leq c_7 (\|\check{\sigma}_1\|_2 + \|\check{\sigma}_2\|_2) \\ \stackrel{(C.8), (C.9)}{\leq} & c_7 \sqrt{\frac{\bar{\varepsilon}^{\mu_\sigma}}{\lambda_\sigma} \widehat{J}_L^*(\check{\xi}_t)} + 2c_7 c_2 \bar{\varepsilon} \sqrt{\frac{\widehat{J}_L^*(\check{\xi}_t)}{\lambda_\beta \bar{\varepsilon}^{\mu_\beta}}} + c_7 p n \bar{\varepsilon}. \end{aligned}$$

This, together with (C.6) and the fact that $J_L^*(\xi_t) \leq \bar{V}$, results in (for some $c_8, c_9, c_{10} > 0$)

$$\|\check{u}^*(t) - u'^*(t)\|_2 \leq c_8 \bar{\varepsilon} + c_9 \bar{\varepsilon}^{\mu_\sigma/2} + c_{10} \bar{\varepsilon}^{1-\mu_\beta/2}. \quad (C.14)$$

C.1.3 Bound on $\|u'^*(t) - \bar{u}^*(t)\|$

Recall again that $u'^*(t)$ and $\bar{u}^*(t)$ correspond to the optimal solutions of two different optimization problems which share the same structure, with the only difference being that the former has an additional term in the cost function; namely $\lambda_\beta \bar{\varepsilon}^{\mu_\beta} \|\check{\beta}(t)\|_2^2$. Following the same arguments as in [9], such a problem can be reformulated into a strongly convex quadratic program (due to Assumption 1) and a bound of the form $\|u'^*(t) - \bar{u}^*(t)\| \leq c_{11} \bar{\varepsilon}^{\mu_\beta/2}$, for some $c_{11} > 0$, is derived. We omit the steps here for brevity, since the analysis follows similar steps. Combining this together with (C.13) and (C.14) yields

$$\begin{aligned} \|\widehat{u}^*(t) - \bar{u}^*(t)\|_2 & \leq \|\widehat{u}^*(t) - \check{u}^*(t)\|_2 + \|\check{u}^*(t) - u'^*(t)\|_2 \\ & \quad + \|u'^*(t) - \bar{u}^*(t)\|_2 \leq \phi_3(\bar{\varepsilon}), \quad (C.15) \end{aligned}$$

for some $\phi_3 \in \mathcal{K}_\infty$, which results from the sum of the three \mathcal{K}_∞ functions (in $\bar{\varepsilon}$).

C.2 Recursive feasibility and inherent robustness of the multi-step nominal eDDPC scheme

We now consider that the system \mathcal{B} is controlled by an n -step nominal eDDPC scheme (as in (7)), but where the input applied to the system is perturbed from the optimal solution, i.e., $u_{[t, t+n-1]} = \bar{u}_{[0, n-1]}^*(t) + \delta_{[t, t+n-1]}$, where $\|\delta_t\|_2 \leq \bar{\delta}$ for all $t \geq 0$. The idea is that one can view the robust scheme with measurement noise (24) as a nominal scheme (7) with bounded input disturbance as shown in (C.15). If such a scheme is feasible at time t , recursive feasibility can be established using standard arguments from model-based MPC, i.e., by defining a candidate solution at the next time step using the previously optimal solution and suitably appending the predicted inputs by a deadbeat controller (which exists due to controllability assumption and that $0 \in \text{int}(\mathbb{W})$). For brevity, we omit this here as it follows similar steps as in [9, Prop. IV.1]. Practical stability is established using Lyapunov arguments. In particular, the Lyapunov function $V(\xi_t)$ in (26) can be bounded as follows

$$c_{V_1} \|\xi_t\|_2^2 \leq V(\xi_t) \leq c_{V_2} \|\xi_t\|_2^2, \quad (C.16)$$

where $c_{V_1} := \frac{\lambda_{\min}(X)}{c}$ and $c_{V_2} := \left(c_J + \frac{\lambda_{\max}(X)}{c}\right)$. For the n step decrease condition, notice that

$$\begin{aligned} & V(\xi_{t+n}) - V(\xi_t) \\ & = J_L^*(\xi_{t+n}) - J_L^*(\xi_t) + \frac{1}{c} (V_{\text{IOSS}}(\xi_{t+n}) - V_{\text{IOSS}}(\xi_t)) \\ & \leq -\|w_{[t, t+n-1]}\|_{\bar{W}}^2 + \phi_4(\bar{\delta}) + \frac{1}{c} (V_{\text{IOSS}}(\xi_{t+n}) - V_{\text{IOSS}}(\xi_t)), \end{aligned} \quad (C.17)$$

where $\bar{W} = \text{diag}(W, \dots, W)$. The first term in (C.17) appears due to the definition of the shifted candidate solutions at time $t+n$, whereas the second term (with $\phi_4 \in \mathcal{K}_\infty$) accounts for the input disturbances. The last term in (C.17) can be bounded by repeatedly applying IOSS arguments (see (25)) to obtain

$$\begin{aligned} V_{\text{IOSS}}(\xi_{t+n}) - V_{\text{IOSS}}(\xi_t) & \leq -\|\xi_{[t, t+n-1]}\|_2^2 + c \|w_{[t, t+n-1]}\|_{\bar{W}}^2 \\ \stackrel{(C.16)}{\leq} & -\frac{1}{c_{V_2}} V(\xi_t) - \|\xi_{[t+1, t+n-1]}\|_2^2 + c \|w_{[t, t+n-1]}\|_{\bar{W}}^2 \end{aligned}$$

Dropping the second term (since it is non-positive), and plugging back into (C.17), we obtain

$$V(\xi_{t+n}) \leq \left(1 - \frac{1}{cc_{V_2}}\right) V(\xi_t) + \phi_4(\bar{\delta})$$

where $\left(1 - \frac{1}{cc_{V_2}}\right) < 1$. Clearly, there exists some $c_{V_3} \in (0, 1)$ such that $\left(1 - \frac{1}{cc_{V_2}}\right) \leq c_{V_3}$ and, hence,

$$V(\xi_{t+n}) \leq c_{V_3} V(\xi_t) + \phi_4(\bar{\delta}). \quad (C.18)$$

C.3 Practical stability of the n -step robust eDDPC

As shown above, an n -step robust scheme based on (24) can be seen as a nominal scheme (7) with bounded input disturbance. Such a scheme is recursively feasible and practically stable. Further, we have previously shown in Section C.1 that the difference between the optimal input of (7) and that of (24) at time t is bounded by a \mathcal{K}_∞ function which depends on the noise level (see, (C.15)). Therefore, one can use Lyapunov arguments to show stability of the n -step robust eDDPC scheme (24). Specifically, (C.16) still holds (which is (27)) as in the previous section. The decay condition (28) can be obtained by combining (C.15) and (C.18), with $\phi := \phi_4 \circ \phi_3 \in \mathcal{K}_\infty$. Finally, for sufficiently small $\bar{\varepsilon} \leq \varepsilon^*$, and due to $V(\xi_t) \leq \bar{V}$, inequality (C.18) can be further bounded by $V(\xi_{t+n}) \leq \bar{V}$. Therefore, by repeatedly applying the same arguments, (28) holds for $t = in, i \in \mathbb{N}$. ■